PART I

PRELIMINARIES

CHAPTER 1

BASICS OF WIND ENERGY CONVERSION SYSTEMS (WECS)

1.1 INTRODUCTION

Renewable energy sources such as solar, wind, hydro, geothermal, tidal, and wave have emerged as a new paradigm to fulfill the energy needs of our civilization. In contrast to fossil fuels, renewable energy sources are clean, abundant, naturally replenished, available over wide geographical areas, and have less or no impact on the environment. Renewable energy sources are primarily used for electricity generation, heating, transportation fuels, and rural energy supply. Electricity production from renewable energy sources has come under growing attention in recent decades. Approximately 22% of global electricity consumption is compensated by all types of renewable energy sources. Driven by technological innovations, cost reduction, government incentive programs, and public demand for clean energy, wind energy is increasingly becoming mainstream, competing with not only other renewable energy sources but also with conventional fossil fuel-based power generation units [1]. At the end of 2014, global cumulative wind power capacity reached 370 gigawatts (GWs), which accounts for approximately 4% of the world's net electricity production [2–4].

Wind energy has been harnessed by mankind for millennia to carry ships across oceans, pump water, and grind grain. The conversion of wind kinetic energy to electric energy started during the 1880s with an automated wind turbine (WT) equipped with a 12-kilowatt (kW) direct-current (DC) generator. To generate electricity from WTs more efficiently and reliably, many improvements have been made in the design of the mechanical and electrical apparatus of WTs. The WT expertise has reached an adequate maturity level by

Model Predictive Control of Wind Energy Conversion Systems, First Edition. Venkata Yaramasu and Bin Wu.

Companion Website: www.wiley.com/go/yaramasu_wu_mpc_wecs

the 1980s, leading to the commissioning of the first 50-kW utility-scale WTs. Over the past 35 years, the size of WTs has gradually increased and has currently reached a massive level of 10 megawatts (MWs). Due to the rapid integration of wind power into the electric grid, many concerns have emerged on the stable and secure operation of existing electric power systems. Grid code requirements have been updated and enforced in many countries on the grid connection of large-scale WTs and wind farms (WFs).

Power electronic converters have been used in commercial WTs since the beginning of grid-connected operation; this technology has significantly evolved over the years [1, 5]. Various combinations of wind generators and power converters have also been developed in commercial WTs to achieve fixed-speed, semi-variable-speed, and full-variable-speed operations. Fixed-speed WT (FSWT) technology, which uses a power converter for the startup function (soft-start), is considered obsolete. Variable-speed WTs (VSWTs) process the electric output power of a generator through a power converter and offer enhanced wind energy conversion efficiency, power quality, and compatibility with grid codes. To fulfill various technical, operational, and grid code requirements, several generator–converter configurations have been developed for commercial WTs.

In addition to the power converter equipment, control system development is important in the safe, successful, and efficient operation of VSWTs. The electrical control system is used to control wind generators and power converters such that maximum energy is extracted from the wind and feeds the energy to the utility grid with high power quality. Electrical control systems are commonly implemented by digital control platforms such as microcontroller (μC), digital signal processor (DSP), or field programmable gate array (FPGA). With the evolution of digital control expertise, the realization of advanced and high-performance control algorithms is now possible. The finite control-set model predictive control (FCS-MPC) is a new breed of digital control technique for power converters and electric generators [6–8]. FCS-MPC opens the doors for controlling WT electric power conversion systems in an easier and more intuitive manner than traditional hysteresis and linear control techniques while offering optimal control performance. This book deals with the FCS-MPC (simply called model predictive control or MPC from here onwards) of power electronic converters in variable-speed WECS.

Chapter Overview

- An overview of wind energy technology is given in Section 1.2 with respect to the installed wind power capacity, wind kinetic energy to electric energy conversion theory, and various classes of WT technologies.
- In Section 1.3, the major mechanical, electrical, and control-related components of the grid-connected high-power WECS are presented. The grid code requirements for large-scale WECS are examined in Section 1.4.
- Fixed speed, semi-variable-speed, and full-variable-speed (Types 1 to 5) WECS are analyzed and compared in Section 1.5. An overview of the broad range of power converters employed in Types 3 and 4 WECS are presented in Section 1.6.
- Section 1.7 presents the control of WECS including pitch control, maximum power point tracking (MPPT) control, grid integration, and taxonomy of wind generator and power converter control. Section 1.8 outlines the main features and challenges of FCS-MPC. In Section 1.9, the linear and model predictive control schemes for variables-speed WECS are presented to demonstrate the simplicity of MPC over traditional control.
- The concluding remarks of this chapter are given in Section 1.10.

1.2 WIND ENERGY PRELIMINARIES

In this section, wind energy preliminaries are discussed briefly in terms of installed wind power capacity, wind energy installations by various countries, wind kinetic energy to electric energy conversion, and evolution of major WT technologies since the 1980s.

1.2.1 Installed Wind Power Capacity

Wind energy is one of the fastest growing renewable energy sources and continues to flourish each year in many countries. The cumulative and annual installed wind power capacities worldwide are shown in Figures 1.1 and 1.2, respectively. The top 10 countries in cumulative and annual installed wind power capacities are shown in Figures 1.3 and 1.4, respectively. Data are presented collectively according to the Global Wind Energy Council 2015 report [2], REN21 renewable global status report 2014 [3], and BTM wind report summary 2015 [4]. The key observations in the installed wind power capacities are summarized below.

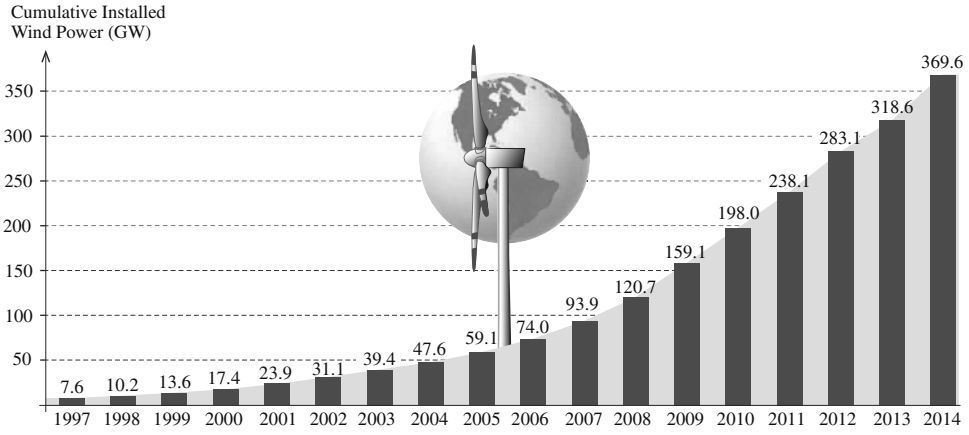

Figure 1.1 Global cumulative installed wind power from 1997 to 2014 [2].

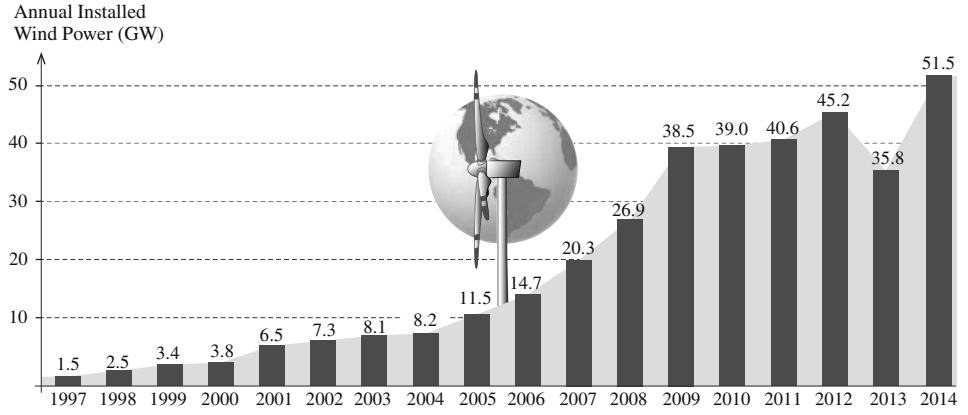

Figure 1.2 Global annual installed wind power from 1997 to 2014 [2].

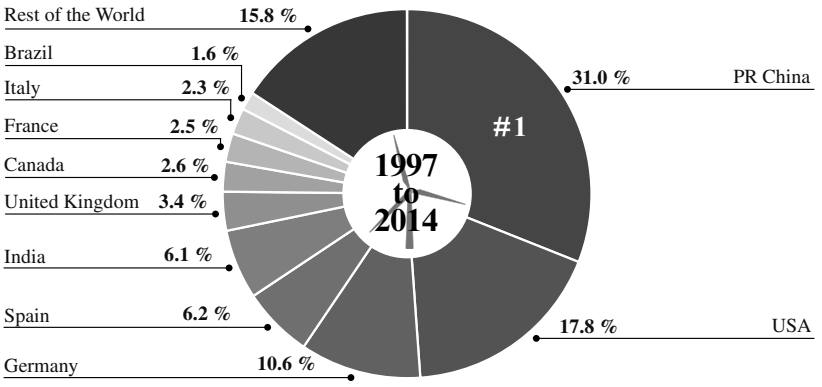

Figure 1.3 Top 10 countries in the cumulative installed wind power by December 2014 [2].

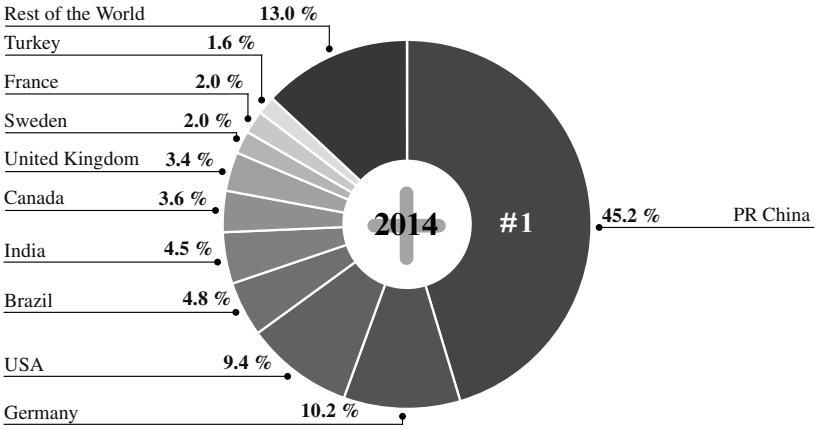

Figure 1.4 Top 10 countries in the new installed wind power from January to December 2014 [2].

- As highlighted in Figure 1.1, the cumulative installed wind power capacity increased exponentially from 7600 MW in 1997 to 369.6 GW by 2014. The data show a cumulative growth rate of 16%. According to the current trend, the cumulative wind capacity is anticipated to reach 600+ GW by 2018.
- The global annual installed wind power capacity in 2014 was 51 GW, which represents a 42% growth over 2013 and investments of approximately USD 99.5 billion.
- Wind energy is present in more than 80 countries, with 225,000+ WTs spinning.
- Approximately 24 countries have more than 1 GW of cumulative installed wind power capacity: 16 in Europe, 4 in the Asia-Pacific region (China, India, Japan, and Australia), 3 in North America (Canada, Mexico, and USA), and 1 in Latin America (Brazil).
- Six countries have more than 10 GW of cumulative installed capacity including PR China (115 GW), the United States (66 GW), Germany (39 GW), Spain (23 GW), India (23 GW), and the United Kingdom (12 GW). These countries represent approximately 75% of global wind energy capacity.
- Asia and Europe are key players in the wind energy industry and host 37.3% and 23.7% of global wind power capacity, respectively.

- Wind power accounts for approximately 4% of the world's net electricity consumption. Wind power has the highest penetration in some countries. For example, 39% of all electricity needs in Denmark is covered by wind power plants.
- The Chinese wind market maintained its top position in both global cumulative and annual installed power by doubling its capacity from 62 GW in 2011 to 115 GW by the end of 2014. PR China has added over 23 GW of new capacity in 2014, which accounts for 45% of the global annual installed capacity and is a record-high number.
- The United States is the second largest country in global cumulative installed capacity. This country added 4.8 GW of new capacity in 2014. Germany and Spain are the third and fourth top countries in wind power, respectively.
- India is the fifth largest country with a cumulative installed wind power capacity of 22.5 GW, which accounts for 6.9% of its electricity consumption. The United Kingdom holds the sixth position with 3.4% installed wind power capacity.
- The cumulative installed wind power capacity in Canada steadily increased from 137 MW in 2000 to 9.7 GW by the end of 2014, thus making it the seventh largest country in wind power. In 2014, 1871 MW of new wind capacity came online in Canada. Currently, 5% of electricity in Canada is covered by wind energy and has ambitious plans to supply 20% of net electricity from wind power by 2025.
- The last three positions in the top 10 lists are occupied by France, Italy, and Brazil.

1.2.2 Wind Kinetic Energy to Electric Energy Conversion

As illustrated in Figure 1.5, WTs convert kinetic energy into electric energy by using various mechanical and electrical components. This section discusses the concept of converting wind kinetic energy to electric energy.

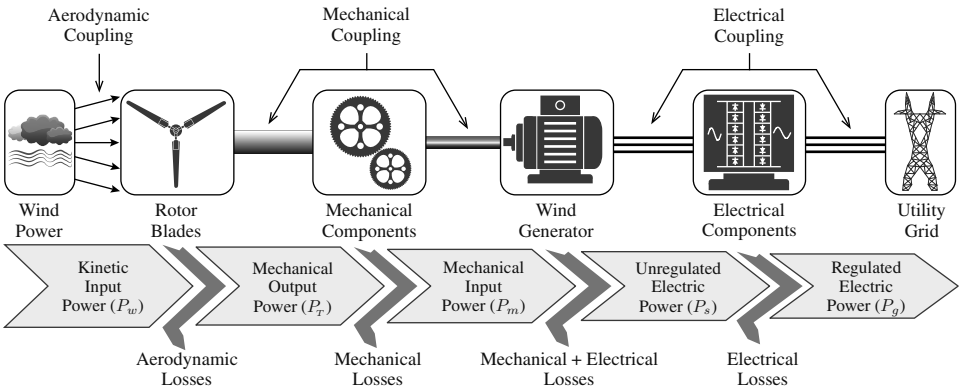

Figure 1.5 Block diagram of wind kinetic energy to electric energy conversion system.

Kinetic energy is first converted into mechanical energy by the rotor blades. The wind kinetic power P_w flowing through an imaginary area A_T at a speed v_w is

$$P_w = \frac{1}{2}\,\rho\, A_T\, v_w^3, \qquad A_T = \pi\, r_T^2 \tag{1.1}$$

where ρ is air density (kg/m^3), A_T is the rotor swept area (m^2), r_T is the blade radius (m), and v_w is the wind speed (m/s). Air density is a function of altitude, temperature, and humidity. At sea level and at 15°C, air has a typical density of 1.225 kg/m^3.

According to the theory of German scientist *Albert Betz*, mechanical power P_T extracted from the wind kinetic power P_w is given by the following:

$$P_T = P_w \times C_p = \frac{1}{2}\,\rho\, A_T\, v_w^3\, C_p \tag{1.2}$$

where C_p represents the power coefficient of rotor blades. The P_T extraction increases in proportion to the C_p value. According to *Betz*, the theoretical or maximum value of C_p is 16/27 or 0.593. For the new generation of high-power WTs, the C_p value ranges between 0.32 and 0.52. The C_p value for various commercial WTs can be found in [9].

The P_w and P_T curves of a WT, with respect to the wind speed v_w, are plotted in Figure 1.6. The value of P_T is always lower than the P_w value because of aerodynamic power losses. The typical cut-in, rated, and cut-out wind-speed values are in the range of 3–5 m/s, 10–15 m/s, and 25–30 m/s, respectively. WTs produce negligible power when wind speed is below the cut-in value; thus, such turbines are usually kept in parking mode. To ensure safety, the turbine is shut down and kept in parking mode when wind speed is above the cut-out value or during emergency conditions. For wind-speed values between cut-in and rated, the P_T curve maintains a cubic relationship with respect to v_w. When wind speed is between the rated and cut-out value, the turbine output power P_T is regulated to its highest threshold (rated) value by the aerodynamic power control.

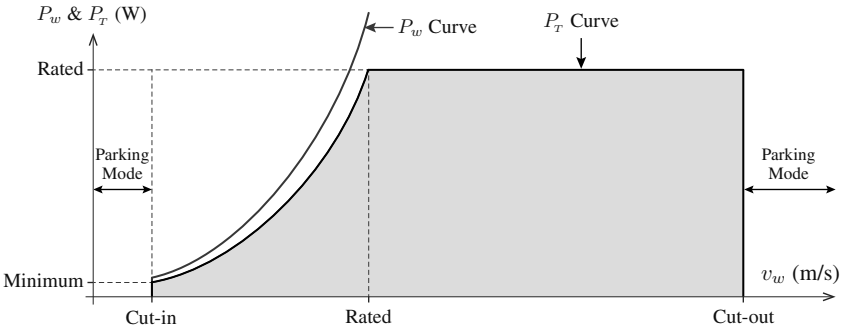

Figure 1.6 WT power characteristic curves with respect to wind speed.

For example, let us consider that a commercial 3.0 MW WT operates with ρ = 1.225 kg/m^3, r_T = 43.36 m, v_w = 12 m/s, and C_p = 0.48. These values are verified as

$$P_T = \frac{1}{2}\,\rho\,\pi\, r_T^2\; v_w^3\, C_p = 0.5 \times 1.225 \times 3.14159 \times 43.36^2 \times 12^3 \times 0.48 = 3.0 \text{ MW}. \tag{1.3}$$

Actual kinetic wind power is $P_w = P_T/C_p$ = 6.25 MW. The slow rotating (5–20 rpm) turbine rotor is mechanically coupled to the fast rotating (1500–1800 rpm) wind generator through the main shaft and drivetrain. Losses in the mechanical components represent the difference between P_T and P_m. The mechanical input power P_m is converted into electric power P_s by the wind generator.

The generator output power P_s is considered unregulated because the generator output voltage and frequency varies according to the wind speed. To feed electric power P_g to the utility grid with fixed voltage and frequency, while complying with the grid code requirements, a power converter is used. To connect the WTs to the utility transmission network, the output voltage of the power converter is boosted usually from 690 V to 33 kV by using a step-up transformer. A more detailed discussion about the mechanical and electrical components of the WT is given in Section 1.3.

1.2.3 Classification of Wind Energy Technologies

As shown in Figure 1.7, in the present wind energy industry, major WT technologies are classified according to various criteria/factors [10]. The most prominent classification factors are based on the following: (1) WT electric output power rating (low, medium, and high power), (2) aerodynamic power regulation scheme during high-wind-speed conditions (stall and pitch control), (3) alignment of wind generator shaft with respect to the ground (vertical and horizontal axis), (4) type of application to feed the turbine electric output power (standalone and grid-connected), (5) wind generator operating speed with respect to the varying wind speeds (fixed and variable speed), (6) location for erection of WTs (onshore and offshore), (7) type of mechanical coupling between the turbine and generator shaft (geared and gearless), and (8) wind-speed velocities (low, medium, and high) affecting the WT. This section provides a brief overview of the various types of predominant wind energy technologies. The other insignificant classification factors are ignored in the analysis.

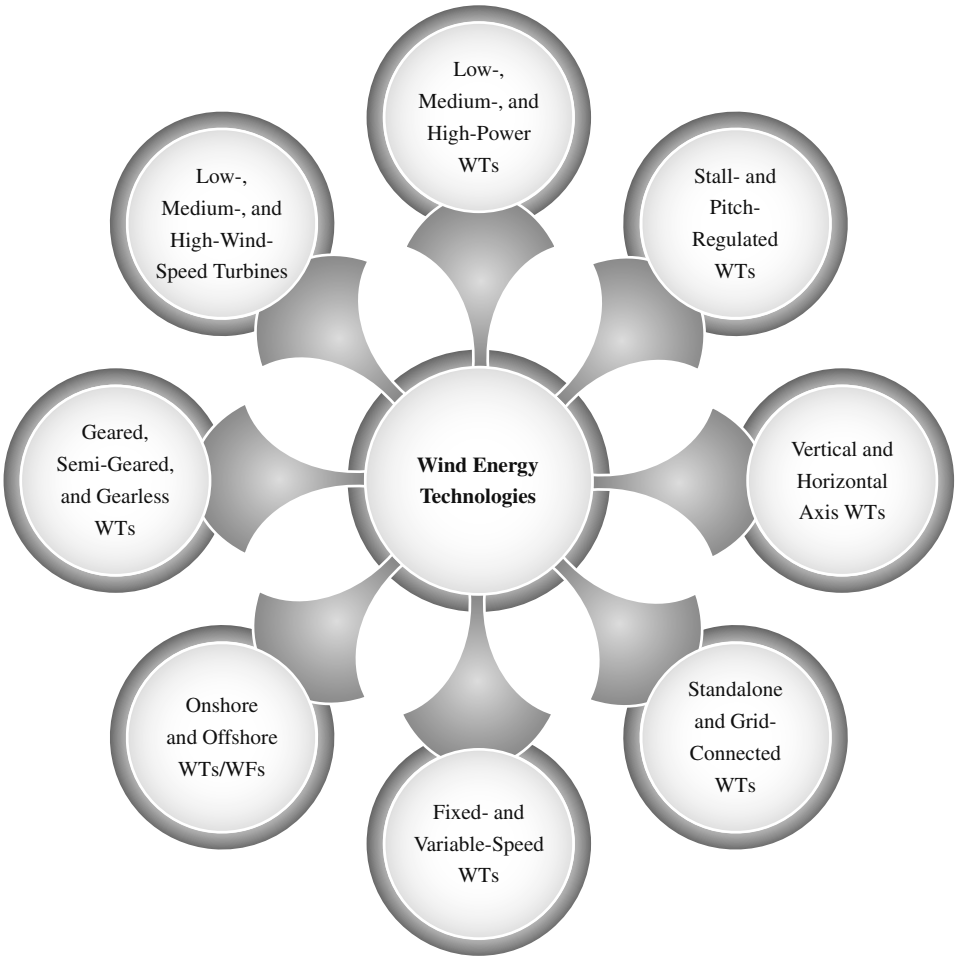

Figure 1.7 Major types of prevailing wind energy technologies.

(1) Low-, Medium-, and High-Power Turbines: According to the nominal electric output power capacity, WTs are classified into three major categories:

- **Low-Power (<30 kW) Turbines:** These turbines are primarily used for battery charging in remote areas, and household electricity generation.
- **Medium-Power (30 to 300 kW) Turbines:** These turbines are used in distributed generation (DG) in conjunction with other renewable energy sources and energy storage systems to supply the electricity needs of small communities.
- **High-Power (>300 kW) Turbines:** These turbines are primarily deployed in wind farms for bulk electricity generation.

By referring to Equation (1.2), $P_T \propto \rho r_T^2 v_w^3 C_p$. Turbine output power can be increased as follows: (1) selecting a turbine erection site with high ρ value, (2) increasing rotor radius size r_T (P_T increases fourfold when r_T is doubled), (3) selecting a site with strong wind speeds or by increasing the tower height to access stable wind speeds (P_T increases eightfold when v_w is doubled), and (4) designing turbine rotor blades with high C_p value. Considering these facts, the size of commercial WTs has exponentially increased over the past 35 years (Figure 1.8). Moreover, large turbines can capture higher wind power with lower installation and maintenance costs than a group of small turbines.

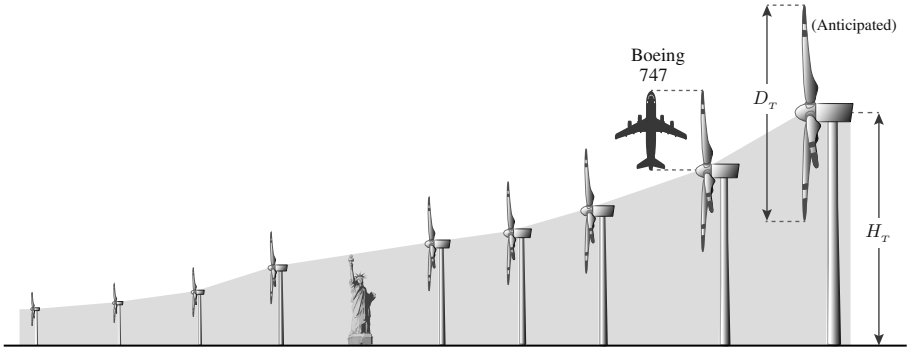

	1980	1985	1990	1995	Statue	2000	2005	2010	2015	2020
P_T (MW)	0.05	0.1	0.5	0.8	of	2	5	7.5	10	15-20
D_T (m)	15	20	40	50	Liberty	124	126	127	190	200-250
H_T (m)	24	43	54	80	93	104	114	135	180	200-250

Figure 1.8 Evolution in the commercial WT size (P_T, rated turbine output power; D_T, turbine rotor diameter; H_T, hub height).

Turbine power capacity increased from 50 kW in 1980 to 10 MW in 2015 [1]. WT rotor diameter also increased from 15 m in 1980 to 190 m in 2015. The largest WT reported by 2015 is 10 MW (`Windtec-AMSC SeaTitan`) with a rotor diameter of 190 m, which is equal to twice the length of a Boeing 747 airplane. Global WT manufacturers such as `Clipper`, `Sway Turbine`, `Sinovel`, `Mitsubishi`, `Goldwind`, `Mecal`, `MingYang`, `United Power`, `GE Energy`, and `Gamesa` have announced their future projects in the 10–15 MW class. The average power rating of WTs installed during 2014 was 1.958 MW. The interest of manufacturers in multi-MW turbines has continued to increase, and turbines rated above 2.5 MW represents 18.5% of all 2014 installations [4]. This book mainly deals with high-power WTs, particularly at the megawatt power level.

(2) Passive Stall-, Active Stall-, and Pitch-Regulated Turbines: By theory, wind turbines can produce more power than the rated (nameplate) value when the wind speed v_w is above its rated value. However, to guarantee secure and reliable function and avoid the overloading of turbine blades, the turbine mechanical output power P_T must be limited to its rated value during strong wind-speed conditions. This process is usually achieved by aerodynamic power control, which manipulates the flow of air stream over rotor blades. Three aerodynamic power regulation methods are available: passive stall, active stall, and pitch control [11]. The characteristics of mechanical output power limitation by these three control methods are depicted in Figure 1.9.

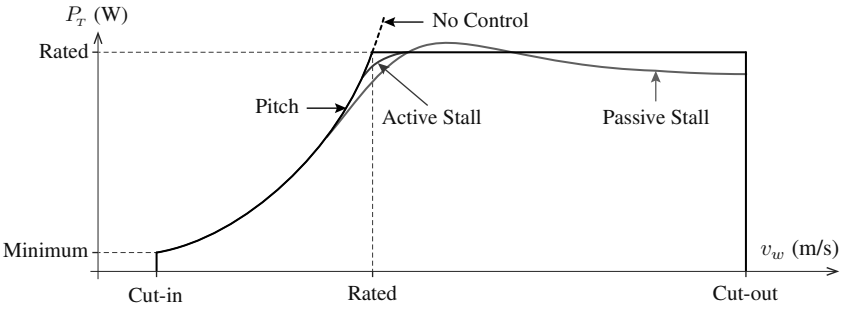

Figure 1.9 Aerodynamic power regulation of WTs by different control methods [11].

The passive stall or simply stall control is the first-generation power regulation method employed for WTs and is the simplest method among the three classes. This approach does not use any sensors, electronic controller, or actuator, thus making it less expensive and robust. In stall-regulated turbines, the rotor blades are firmly fixed (bolted) to the rotor hub at a fixed angle. When wind speed increases beyond a certain limit (for example, 15 m/s), the turbulence created on the rotor surface causes the airfoils to lose lift force, thus decreasing the power captured from the wind. P_T exceeds the rated value with an overshoot at a certain wind speed. The overshoot in P_T is an undesirable function. As v_w increases above the rated value, P_T gradually decreases, thus leading to low energy conversion efficiency. Passive stall control is used in low- to medium-power WTs.

Active stall control is an advanced version of passive stall control with adjustable rotor blades. When v_w increases above the rated value, P_T is reduced by moving (pitching) the blades into the wind, thus causing turbulence (stall mechanism) over the blades. This approach improves wind energy conversion efficiency at low wind speeds and ensures that P_T does not exceed the rated value during high-wind-speed conditions (refer to Figure 1.9). This method is employed in medium- to high-power WTs.

In pitch-regulated turbines, the rotor blades are adjustable similar to active stall turbines. The pitch control mechanism is assisted by an electronic controller and motor (or hydraulic) drives. During high wind speeds, the electronic controller sends a control signal to the motor to turn the rotor blades along the longitudinal axis (pitching) such that angle of attack of the blades is reduced. The active stall method turns the blades "into wind" to create a stall mechanism, whereas pitch control turns the blades "out of wind." The mechanical output power is tightly regulated by the pitch control as highlighted in Figure 1.9. This control provides faster responses/actions than the passive stall and active stall controls and is extensively used in modern high-power WTs [12]. Unless otherwise stated, the default aerodynamic power regulation employed in this book is pitch control.

(3) Vertical and Horizontal Axis Turbines: In the present wind industry, two basic types of WTs are available depending on the orientation of the wind generator and drivetrain shaft with respect to the ground: vertical-axis WTs (VAWTs) and horizontal-axis WTs (HAWTs) [13]. Both WT types convert wind kinetic energy into electric energy but have different spinning axes with respect to ground.

In VAWTs, the shaft of wind generator is placed perpendicular to the ground. The turbine rotor is implemented by vertically mounted curved airfoils with different designs for rotor shapes. The installation and maintenance of VAWTs is easier than HAWTs because the generator and gearbox are placed close to the ground. VAWTs accept wind from any direction; thus, the orientation of the WT blades is not necessary. The rotor shaft is usually long and is more prone to mechanical vibrations. The rotor blades are subjected to uneven wind speeds: strong at the top and weak at the bottom. Therefore, wind energy conversion efficiency is lower with VAWTs than with HAWTs. The aerodynamic power regulation of VAWTs is complicated and is unsuitable for high-power applications.

In HAWTs, the wind generator shaft is placed horizontally to the ground. Major mechanical and electrical components are placed in a nacelle, and the tower elevates the height of the nacelle to allow sufficient space for the blades to rotate. Three rotor blades are commonly used in commercial HAWTs. The rotor blades are subjected to strong winds because of the elevated height; thus, HAWTs offer high-wind-energy conversion efficiency. The initial and maintenance cost of HAWTs is higher than VAWTs because the blades, gearbox, and generator of the former are placed away from the ground. Furthermore, HAWTs have easier aerodynamic power regulation and lower mechanical vibrations than VAWTs. HAWTs are predominantly used in medium- and high-power applications, and this book considers the HAWT technology only.

(4) Standalone and Grid-Connected Turbines: According to the type of application to feed electric output power, WTs are classified as standalone and grid-connected systems. Standalone DG is an alternative solution to power consumers in locations wherein the expansion of the electric grid is prohibitive and expensive. In standalone DG, load demand varies with respect to time and turbine output power changes with respect to wind speed. To provide stable, secure, and reliable electricity, WTs are used in conjunction with other power generation units such as photovoltaic (PV), mini/micro hydro, biomass, and diesel generators, as well as energy (usually battery energy) storage systems [14]. Low- to medium-power WTs are commonly employed in standalone applications and represent only a fraction of global cumulative installed wind power capacity.

Low- and medium-power WTs can also be used in grid-connected DG to reduce electricity consumption from the utility grid. When the electricity produced by the WT exceeds the household or community requirements, the electricity is sold to the utility without employing any energy storage. By contrast, the majority of commercial high-power WTs are employed in grid-connected applications. The power produced by high-power WTs is fed directly into the grid. The output of WTs is usually less than 1000 V but is boosted to a few kV by using a step-up transformer to send power via transmission lines. Wind farm power is fed into a grid by high-voltage alternating current (HVAC) or high-voltage direct current (HVDC) transmission lines. The power to be delivered and the distance of the wind farm to the nearby utility grid are two crucial factors that play an important role in deciding between HVAC and HVDC transmission. HVAC transmission is favorable for small-scale wind farms, which are located close to the utility grid. For power ratings and distances greater than 400 MW and 60 km, respectively, HVDC transmission is an excellent choice [15]. This book mainly deals with grid-connected high-power WTs.

(5) Fixed-Speed and Variable-Speed Turbines: On the basis of rotational speed, grid-connected turbines are classified as FSWTs and VSWTs. To aid in the discussion, tip speed ratio (TSR), which is a vital WT design parameter, is introduced here. TSR is defined as the ratio between the tangential speed of the blade tip and the wind speed [11]:

$$\lambda_T = \frac{\omega_T \, r_T}{v_w} \tag{1.4}$$

where ω_T is the angular speed of the turbine (rad/s) and v_w is the wind speed (m/s).

The power coefficient C_p discussed in (1.2) is a function of the TSR and blade pitch angle. The C_p versus λ_T curve is shown in Figure 1.10(a) when the pitch angle is held at a rated (zero) value. At a rated wind speed $v_{w,R}$, both FSWT and VSWT operate at an optimal TSR, λ_T^{op}, and maximum (optimal) power coefficient, C_p^{op}. The turbine output power P_T corresponding to the rated wind speed is also maximum (Figure 1.10(b)).

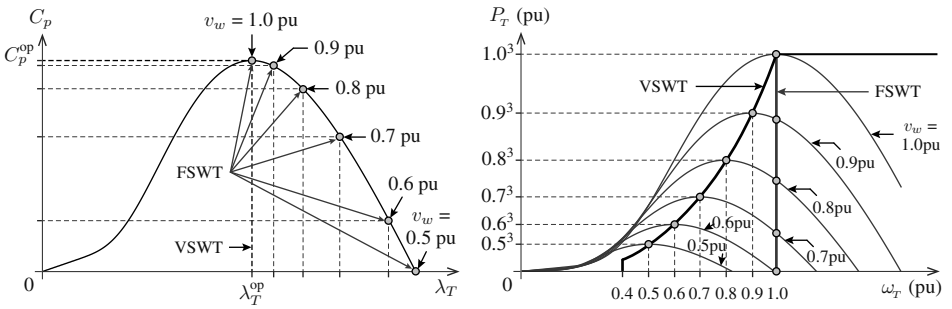

(a) C_p versus λ_T curve (b) P_T versus ω_T curve

Figure 1.10 Characteristics of FSWT and VSWT during different wind-speed conditions.

The first generation of grid-connected WTs developed during the 1980s were based on fixed-speed technology. These WTs are connected to the utility grid directly without any power converter, thus making the FSWT configuration simple and cost effective. In FSWTs, the wind generator operates at an almost constant speed, regardless of the wind speed. In FSWTs, the speed ω_T is decided according to the gear ratio, number of poles in the wind generator, and grid frequency. By referring to (1.4), the TSR value (λ_T) increases when wind speed v_w decreases at a constant ω_T. According to the WT characteristics, power coefficient C_p decreases when λ_T increases (Figure 1.10(a)). As demonstrated in Figure 1.10(b), the turbine output power P_T also decreases rapidly because of the reduction in both C_p and v_w. With the fixed-speed operation, the wind energy conversion efficiency decreases and mechanical stress on the drivetrain increases.

In VSWTs, the rotor speed ω_T is changed according to the wind speed v_w, such that the turbine always operates at an optimal TSR value λ_T^{op}. For example, when the wind speed changes to 0.9 pu, the turbine/generator speed ω_T also changes to 0.9 pu. Given this, C_p value is maintained at an optimal value, C_p^{op}, and P_T always holds a cubic relationship with v_w. Therefore, wind energy conversion efficiency in VSWTs is higher than with FSWTs (see Figure 1.10(b)). The initial cost of VSWTs is high because of the power converter; however, the high-energy yield of the VSWTs compensates the high initial cost and power losses in the converter. In the present wind energy industry, VSWTs are dominantly used. This book mainly deals with variable-speed WTs.

(6) Onshore and Offshore Turbines/Farms: A group of WTs is often placed over an extended area to form a wind farm and is connected to a national electric grid. Wind farms can be located on the land (onshore) or in the sea (offshore). Traditionally, onshore wind farms have been developed for the ease of construction, low initial and maintenance costs, improved proximity to transmission lines, and low-power transmission losses [1].

Nowadays, offshore wind farms are gaining more attention because power production can be increased and stabilized with the help of strong and steady winds. Furthermore, the effect on land use and landscapes can be reduced, audible noise and visual impacts can be mitigated, and opposition by "Not in My Back Yard (NIMBY)" movement will be low. The initial and maintenance costs of offshore wind farms are higher than onshore wind farms for the same power levels because stronger foundations are needed and connections to the onshore grid require submarine AC or DC cables (buried deep under the ocean floor). Offshore technology is another important driving force behind the amazing growth size in WTs (refer to Figure 1.8 on page 10). In 2013, the average power ratings of onshore and offshore WTs were reported to be 1.926 and 3.613 MW, respectively.

The global cumulative installed offshore wind power capacity is displayed in Figure 1.11. The offshore installed capacity increased exponentially from 29 MW in 1997 to 8771 MW in 2014 [2, 16]. By 2014, offshore wind power accounted for approximately 2% of the total (cumulative) wind power capacity installed around the world. Offshore project proposals and present trends indicate that by 2020, offshore wind power capacity will reach 40 GW [16]. The projected wind power is anticipated to supply approximately 4% of the European Union's electricity demand.

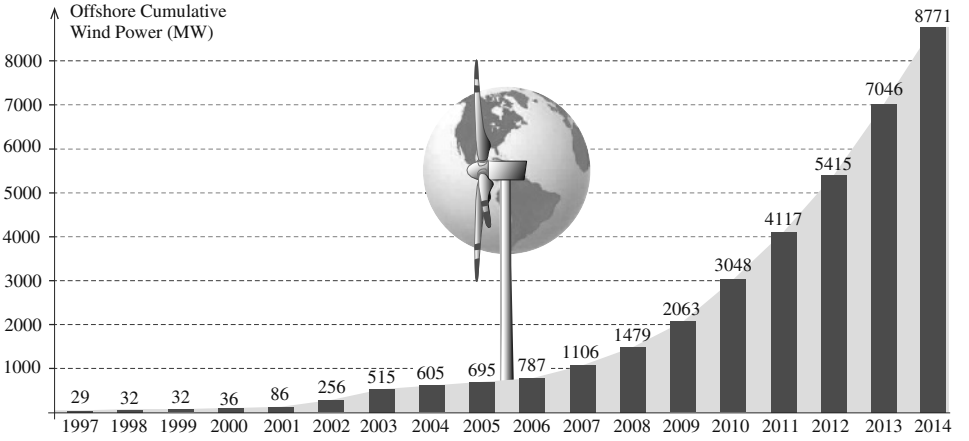

Figure 1.11 Global cumulative installed offshore wind power from 1997 to 2014 [2, 16].

Most offshore projects (nearly three-quarters) are located in European countries. The United Kingdom, Denmark, Belgium, Netherlands, Germany, Sweden, Finland, and Ireland are key players for offshore wind energy in Europe. The largest offshore wind farm to date is the London Array with 630 MW installed capacity. Future offshore wind farms are proposed in the range of 1200–2500 MW. Some of these projects include the following: Blekinge Offshore, Sweden (2500 MW); Korea Offshore, South Korea (2500 MW); and Moray Firth, United Kingdom (1300 MW). This book deals with both onshore and offshore wind energy systems.

(7) Geared, Semi-Geared, and Gearless Turbines: WTs are categorized into three types according to the speed of the wind generator and the type of coupling between the turbine main shaft and wind generator shaft:

- **Geared Turbine:** The low-speed (5–20 rpm) turbine rotor is connected to the high-speed (1500–1800 rpm) wind generator shaft through a three-stage gearbox.
- **Semi-Geared Turbine:** A single- or two-stage gearbox is used to couple the low-speed turbine rotor with the medium-speed (400–600 rpm) wind generator shaft.
- **Gearless Turbine:** The turbine rotor is directly coupled to the generator shaft.

The three-stage gearbox is commonly used in FSWTs and in some VSWTs. This gearbox has several serious issues such as high initial cost, high audible noise, extensive wear and tear, reduced life span, reduced efficiency, and need for regular maintenance [17]. The omission of a gearbox (often referred to as gearless or direct-drive technology) helps overcome the aforementioned problems, particularly in offshore WTs. This concept was first introduced in 1992 by `Enercon`, a German manufacturer, through the E-40/500 kW WT model. In recent years, many turbine manufacturers, such as `Avantis`, `GE Energy`, `Goldwind`, and `Vensys` to name a few, have used direct-drive technology in their commercial products. The direct-drive market in 2014 is 13,740 MW and represents 27% of global WT installations [4].

By contrast, a direct-drive operation leads to some drawbacks in the design of generators, such as large diameter and more weight [18]. To make a compromise between high- and low-speed operations, a medium-speed generator is used in conjunction with a single- or two-stage gearbox. The single-stage gearbox (with a gear ratio of 10) was first introduced by `Multibrid` in their M5000 WT models. Other turbine manufacturers such as `MingYang` and `WinWinD` developed 2-stage gearboxes with a gear ratio of 20–30. This book considers geared, semi-geared, and direct-drive turbines in the analysis.

(8) Low-, Medium-, and High-Wind-Speed Turbines: According to the International Electrotechnical Commission (IEC) 61400-1 standard, WTs are also arranged into different classes on the basis of annual average wind speed, turbulence, and extreme 50-year gust data. The summary of WT classes is shown in Table 1.1. The design and construction phase of wind power plant relies highly on this data to forecast the wind climate that will affect the WTs. All manufacturers provide WT products to meet various IEC classes. For example, `Vestas` offers 3.45 MW WTs in different model numbers to cover various IEC classes: V105-IEC IA, V112-IEC IA, V117-IEC IB/IIA, V126-IEC IIA/IIB, and V136-IEC IIIA.

Table 1.1 Wind turbine classes according to the IEC 61400-1 standard

Wind Class	Annual Average Wind Speed	Turbulence Level	Extreme 50-Year Gust
IA	High Wind Speed – 10 m/s	High Turbulence – 18%	High Gust – 70 m/s
IB	High Wind Speed – 10 m/s	Low Turbulence – 16%	High Gust – 70 m/s
IIA	Medium Wind Speed – 8.5 m/s	High Turbulence – 18%	Medium Gust – 59.5 m/s
IIB	Medium Wind Speed – 8.5 m/s	Low Turbulence – 16%	Medium Gust – 59.5 m/s
IIIA	Low Wind Speed – 7.5 m/s	High Turbulence – 18%	Low Gust – 52.5 m/s
IIIB	Low Wind Speed – 7.5 m/s	Low Turbulence – 16%	Low Gust – 52.5 m/s
IV	6.0 m/s	–	42 m/s

1.3 MAJOR COMPONENTS OF WECS

From the pool of 8 types of WT technologies presented in Section 1.2.3, the following turbine types are considered in order: high-power WT, pitch-controlled WT, horizontal-axis WT, grid-connected WT, variable-speed WT, onshore WT, geared WT, and any IEC class WT. The basic configuration of WT, which integrates the above 8 types of technologies, is depicted in Figure 1.12. A typical MW-WECS is composed of over 8000 components that convert wind kinetic energy into electric energy in a controlled, reliable, and efficient manner. The most visible parts are the tower, nacelle, rotor blades, and step-up transformer. The rest of the components are housed inside the WT. The major components of a WECS are broadly classified into three categories:

- **Mechanical Components:** Includes the rotor blades, rotor hub, rotor bearings, main shaft, mechanical brake, gearbox, pitch drives, yaw drives, wind measurement unit, nacelle, tower, foundation, heat exchange system, and ladder.
- **Electrical Components:** Includes the wind generator, power electronic converter along with generator- and grid-side harmonic filters, step-up transformer, power cables, wind farm collection point, and switch gear.
- **Control Components:** Includes mechanical and electrical-related control systems.

The cost analysis on a REPower (now Senvion) MM92-5.0 MW WT indicates that the costs (in % of total WT cost) associated with major parts are as follows: tower 26.3%, rotor blades 22.2%, gearbox 12.91%, power converter 5.01%, transformer 3.59%, wind generator 3.44%, main frame 2.80%, and pitch drives 2.66% [19]. The costs associated with the wind generator, power converter, and transformer change slightly according to the type of wind energy system configuration. Further details on various WECS configurations will be discussed in Section 1.5.

1.3.1 Mechanical Components

Mechanical components play an important role in the practical development of multi-megawatt WTs. Mechanical components convert wind kinetic energy into mechanical energy and transmit it to the wind generator through the drivetrain. The "rotor" components include rotor blades, rotor hub, rotor bearings, nose cone, and pitch drive. The "drivetrain" includes mechanical coupling, bearings, low-speed main shaft, high-speed generator shaft, gearbox, and mechanical brakes. A brief description of the major mechanical components is given as follows.

(1) Rotor Blades: The wind kinetic energy is first converted to mechanical energy with the help of airfoil-shaped rotor blades. WT blades are the most distinctive, visible, and important components. WT blades look like airplane wings and share the same aerodynamic characteristics because of their structural and aerodynamic behavior. Over the past three decades, WT blade technology has evolved rapidly in terms of aerodynamic design and materials. Older style WTs were designed with heavier steel blades, thus leading to high inertia. Newer turbines use efficient and composite materials to obtain low rotational inertia such that WTs can accelerate quickly if the wind speed increases. The most commonly used materials in modern WTs are fiber-reinforced polymers, aluminum, polyester resin, balsa wood, glass-reinforced plastics, and carbon-fiber composites. The three-blade design is the standard for current MW WTs because it provides symmetrical loading.

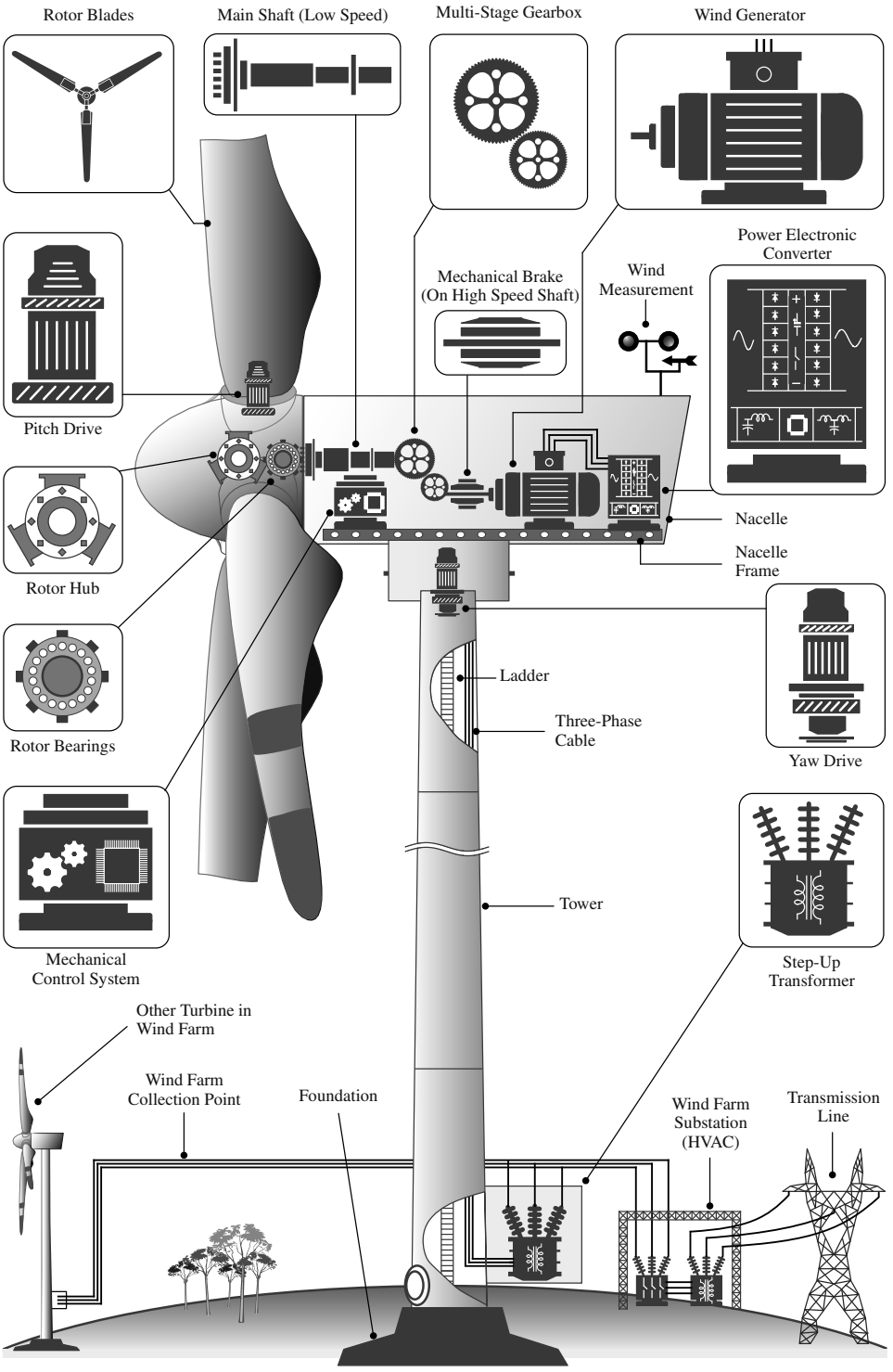

Figure 1.12 Major components of a variable-speed high-power WECS.

Blade requirements such as lighting protection, audible noise reduction, optimum shape, high power-to-area ratio, and ease of manufacturing impose a great challenge to turbine manufacturers. Recent developments in blade sandwich technology can lower manufacturing and transportation costs. WT blades have a maximum aerodynamic efficiency of 59% according to the *Betz* limit. Improving aerodynamic efficiency is of prime importance for mechanical engineers; the highest efficiency achieved to date is 50% in `Enercon`, `Shandong SwissElectric`, and `Wikov` blades [9].

(2) Rotor Hub and Bearings: Rotor hubs made of cast iron or cast steel provide mechanical support to the rotor blades and convert the transverse motion of the blades into torque input for the gearbox. The rotor blades are connected to the rotor hub in different manners according to the type of aerodynamic power control. In older passive stall turbines, the blades are directly bolted to the hub. In modern turbines, a more sophisticated design is used to connect the blades to the hub through pitch drives. The rotor hub also houses the pitch drives or tip brakes. The rotor bearings provide support for coupling between the rotor hub and main shaft besides facilitating the smooth rotation of the later one.

(3) Main Shaft and Mechanical Brake: Given the large moment of inertia, MW WTs usually run at very low speeds (typically 5–20 rpm) and high torque. The main shaft, also referred to as the low-speed shaft, connects the rotor hub to the gearbox for the transmission of mechanical energy. The main shaft is usually made of forged high-carbon steel, cast iron, or cast steel to maintain optimized load transfer.

Mechanical brakes are used to stop the WT in emergencies such as fault conditions (over-heating of gearbox/generator) or high wind gusts. To reduce braking torque, mechanical brakes are mounted directly on the high-speed generator shaft. The brakes can create a huge wear and tear on the shaft, and fire inside the nacelle if used to stop the turbine from full speed. In practice, mechanical brakes are applied after pitch and yaw drives bring the rotor speed to certain low value. Hydraulic or electromechanical disc (or drum) brakes are used in modern high-power turbines.

(4) Gearbox: To couple the "low-speed and high-torque" main shaft with the "high-speed and low-torque" generator shaft, a multi-stage gearbox is used. A 3-stage gearbox containing 1 planetary stage and 2 helical stages is usually employed for high-speed generators. For a 3-stage gearbox, the gear ratios usually vary between 60 and 120 and the gearbox efficiency varies between 95% and 98%. In practice, the gearbox is subjected to a wide range of loading conditions because of the random nature of wind speed. This phenomenon causes extensive wear and tear on the gearbox. Therefore, regular maintenance is needed to ensure a long service life. The gearbox is one of the major sources of WT downtime and requires high maintenance costs, in addition to huge initial investments. Moreover, the gearbox produces a high level of audible noise. Gearless WTs are promising for offshore applications to reduce maintenance cost and downtime.

(5) Pitch and Yaw Drives: As discussed earlier in Section 1.2.3 on page 11, according to aerodynamic properties, any particular turbine generates maximum electricity at or above the rated wind speed only. When wind speed is more than the rated value, the blade angle is changed such that the generator electric output power is limited to the rated value [12]. In large WTs, three independent pitch drives and an electronic controller are used in the rotor hub to rotate the blades along their longitudinal axis. Pitch drives can be implemented by either hydraulic or electric mechanisms, but the latter is commonly used to reduce complexity and maintenance cost and obtain fast pitching rates of 7.5–8°/s.

The yaw drive is used to move the rotor blades and nacelle toward the wind to extract the maximum possible energy. The yaw drive is composed by electric motor drives, yaw gear, gear rim, and bearings and produces high torque to turn the nacelle. When the wind speed is above the cut-out value or when a malfunction occurs, the yaw mechanism helps stop the turbine by moving it out of the wind.

(6) Wind Measurement Unit: WTs are equipped with wind measurement units composed of an anemometer and wind vane to continuously monitor and collect wind data. As mentioned earlier, the pitch and yaw drives require wind speed and direction information, respectively. Electrical control systems also require this information for variable-speed operations. The anemometer consists of a three-cup vertical-axis micro-turbine and a speed transducer to measure wind speed. Ultrasonic anemometers have recently been introduced for WTs to obtain accurate wind data and provide reliable operation compared with mechanical anemometers. A wind vane along with an optoelectronic angle transducer measures the wind direction, and the wind measurement units are usually mounted on the top back part of the nacelle.

(7) Nacelle: The nacelle houses most of the mechanical and electrical components and protects them from extreme weather conditions. The nacelle faces upstream wind during normal operating conditions. The size of the nacelle greatly changes according to the type of gearbox employed. For example, for direct-drive WTs, the nacelle size is small compared with the gearbox-based WT. In recent offshore WTs, a helicopter-hoisting platform is built on top of the nacelle for service personnel to winch down to turbine from a helicopter hovering above it.

(8) Tower and Foundation: The tower, commonly made of steel or concrete, elevates the height of the nacelle and rotor blades to access better wind-speed conditions. The height of the tower increases with the rotor diameter or with turbine power capacity, to allow sufficient clearance from the ground. The requirement for clearance from the ground is higher in onshore WTs than in offshore turbines. In modern turbines, tower height is approximately two to three times the blade length. The power cables (which connect the power converter output to the step-up transformer) and ladder are attached to the inner surface of the tower. In some MW turbines, the step-up transformer and electrical switch gear are also housed inside the tower to reduce space requirements and protect these components from severe weather conditions.

The turbine foundation directly supports the tower, nacelle, and rotor blades. The foundations for onshore turbines are simple and includes slab, monopile and multipile types. Designing the foundations for offshore WTs is a challenging task because of different water depths and soil types, as well as harsh weather conditions. This issue has triggered many research and development activities, and currently many offshore foundation concepts are available such as gravity, monopile, tripod, tripile, jacket, and floating. Gravity and monopile foundations are applicable for shallow waters with depths less than 30 m [20]. Other foundations, particularly floating foundations, which have already been used in offshore oil and gas industries, are promising for future deep water (>40 m) offshore wind farm projects.

(9) Miscellaneous Mechanical Components: Several other miscellaneous components exist that are not directly involved in power conversion. However, they assist the main mechanical components in the operation and maintenance of WTs. These components include the heat dissipation/exchange system, lightning protection system, mechanical vibration dampers, ladder, and service lift.

1.3.2 Electrical Components

(1) Wind Generator: The wind generator converts rotational mechanical-energy input into electric energy output. Over the past 35 years, many generators such as the squirrel-cage induction generator (SCIG), wound rotor induction generator (WRIG), doubly fed induction generator (DFIG), permanent magnet synchronous generator (PMSG), and wound rotor synchronous generator (WRSG) have been developed for WTs [17, 21]. WRIG and DFIG have the same construction process but have different names in literature to distinguish different turbine configurations. The WRSG is also denoted as an electrically excited synchronous generator (EESG) in literature. In an attempt to increase the power density of 10 MW class WTs, high-temperature-superconducting (HTS) synchronous generators (SGs) have been introduced recently in the wind energy industry. HTS-SG eliminates the need for rare earth materials and significantly decreases the size and weight of the generator compared with the standard WRSG/PMSG. AMSC and ABB have announced the use of HTS-SGs in their future 10- and 15-MW WT projects, respectively.

The SCIG is popularly used in first-generation direct grid-connected WTs because of its low cost, simple and rugged construction, and minimum maintenance requirements. The SCIG is also used in present variable-speed MW WECS along with a power converter. An induction generator (IG) with accessible rotor windings (i.e., WRIG and DFIG) enables variable-speed operation by employing a variable resistor or power converter in the rotor circuit. The DFIG is the current workhorse of the wind energy industry with more than 50% market share. The PMSG, WRSG, and HTS-SG are used mainly in direct-drive MW WTs. IGs are used in both fixed speed and variable-speed turbines, whereas SGs are used in variable-speed WECS. IGs operate at high rotational speeds, whereas SGs can operate at low, medium, or high speeds. To achieve low operational speed, the generator needs to be equipped with a large number of poles, which is a feasible solution for SGs. In accommodating the large number of poles, the PMSG stator radius becomes approximately 6 times larger and 4.5 times heavier than three-stage gearbox-based IG [18]. The main features of these generators are summarized in Table 1.2.

Table 1.2 Main features of induction and synchronous wind generators [22, 23]

Generator	Advantages	Disadvantages
SCIG	✔ Simple and rugged construction	✖ Consumes reactive power from grid
	✔ Lower initial and maintenance cost	✖ Limited to high-speed operation only
	✔ Readily available for MW applications	✖ Requires a soft starter to limit in-rush current
WRIG/ DFIG	✔ Rotor power allows variable speed	✖ Initial and maintenance cost is high
	✔ High starting torque capability	✖ Low-power factor (PF) at light loads
	✔ Flexible reactive power control	✖ Slip rings need regular care
PMSG	✔ High power density and reliability	✖ High cost for PM material
	✔ No need for excitation and gearbox	✖ Possible demagnetization of PMs
	✔ Lower rotor losses and high efficiency	✖ Low-speed generators are heavy
WRSG	✔ Independent P and Q control	✖ High capital and maintenance cost
	✔ High-torque operation can be achieved	✖ Requires additional excitation circuit
	✔ Eliminates the need for gearbox	✖ Frequent attention is needed for slip rings
HTS-SG	✔ Significantly compact and light weight	✖ High initial cost
	✔ Lower winding losses	✖ Cooling system design is complicated
	✔ Larger air-gap eliminates tolerance issues	✖ Greater tendency for rotor speed instability

(2) Power Converter: Wind generator output voltage and frequency changes with respect to the rotational speed (wind speed). The generator output terminals can be directly coupled to the grid or can be interfaced through a power electronic converter [24]. The power converter changes the generator AC output voltage to DC voltage by a rectifier (AC/DC converter) and then back to AC with a fixed voltage magnitude and frequency by an inverter (DC/AC converter). In most WTs, the configuration of both AC/DC and DC/AC converters is the same and is known as a back-to-back (BTB) connected converter. By arranging the power switching devices in different ways, possibly with DC-link elements such as capacitors or inductors, numerous power converter topologies can be derived. As shall be introduced in Section 1.5, these power electronic converters can be combined with electric generators to form a wide variety of WECS configurations. Switching harmonics are inevitable when using power converters. To solve this issue, harmonic filters are used in wind machine (generator)-side converters (MSCs) and grid-side converters (GSCs). The harmonic filter in the MSC helps reduce the harmonic distortion of the generator currents and voltages. This process leads to a reduction in harmonic losses incurred in the magnetic core and winding of the generator. The harmonic filter in the GSC helps meet the strict harmonic requirements specified by the grid codes [25].

On the basis of operating voltage, power converters are broadly classified as low-voltage (LV) and medium-voltage (MV) converters. LV or MV operation for a power converter is decided according to the wind generator output voltage magnitude. A low voltage power converter is used with a low voltage wind generator; similarly, a medium voltage power converter is employed with a medium voltage wind generator. The definition of WECS LV and MV operating voltages in the North American and European market is summarized in Table 1.3 [26]. The most popular LV and MV ratings for wind generators (and power converters) are <1000 and 3000–4000 V, respectively. A more detailed discussion on LV and MV power converter topologies for WTs is presented in Section 1.6.

Table 1.3 LV and MV classification by region [26]

Region	Standard	Voltage Class
Europe	IEC 60038	LV (<1000 V) • 220, 400, 690 V MV (1 – 35 kV) • 3.3, 6.6, 11, 22, 33 kV
North America	ANSI C84.1	LV (<600 V) • 208, 120/240, 480, 575 V MV (600 V – 35 kV) • 2.4, 4.16, 6.9, 12.47, 13.8, 21, 34.5 kV

(3) Step-Up Transformer: The power converter output voltage (typically 690 V in LV class) is boosted to 34.5 kV (in North America) by using a step-up transformer to connect the WTs to an MV collection point. The step-up transformer is mandatory in a WT; otherwise, the wind generator and power electronic converter should be designed for WF collection-point voltage level. This approach eliminates the cost of a step-up transformer; however, additional costs are incurred with the MV wind generator and power converter. In the present wind energy industry, all WTs use step-up transformers as the default component. Step-Up transformers are available in two forms: dry transformer (cast resin) and liquid (oil) filled transformer.

(4) Power Cables: The power cables connect the output of the power converter, which is usually located in the nacelle to the step-up transformer, which is placed at the bottom of the WT. The tower pendent LV power cables consist of coated copper and a simple insulation system. The cost, size, and power losses associated with LV power cables increase as the power rating of the LV WT increases. For example, let us consider a 6.0-MW power converter operating at 690 V. The *root-mean-square* (*rms*) value of the three-phase line currents becomes 5020 A, which must be carried by high-current capacity power cables. In some WT designs, the transformer is placed in the nacelle to decrease the cable cost and losses. However, this approach requires the size optimization of other electrical and mechanical components.

Another approach to mitigate the above cable issues is to increase the WT voltage to MV level. For a 6.0-MW turbine, the *rms* value of the line currents significantly decreases to 866 A when a 4000-V power converter is employed and leads to a smaller cable size and lower power losses than LV cables. The construction and termination of MV power cables is complicated, and the salary and wages of MV technicians is higher than LV technicians. However, the aforementioned advantages of MV cables outweigh this drawback.

(5) Wind Farm Collection Point: The wind farm collection point, also referred to as the point of common coupling (PCC), connects all WTs in a wind farm. The parallel connection of WTs is the default practice for increasing the power capacity of the wind farm. The most common PCC voltages employed in North American and European wind farms are 34.5 and 33 kV, respectively. Commercial WTs can be connected to the PCC through step-up transformers, regardless of the regional voltage classes. Thus, given the participation of European manufacturers in North America and vice versa, the regional voltage classifications outlined in Table 1.3 are becoming less important.

(6) Miscellaneous Electrical Components: The miscellaneous electrical components include electric switch gear, three-phase contactor, and circuit breaker, which are connected between the WT and PCC or between the PCC and transmission line.

1.3.3 Mechanical and Electrical Control Systems

WTs are fully automated and operate unmanned yearlong under all weather conditions. The control systems have been used with limited functions in the first generation of WTs, and now they perform a large number of functions with respect to turbine, generator and power converter, grid integration, protection standards, and wind farm operation. In WTs, several slave control systems for the mechanical/electrical components and a master control system are used in a cooperative manner to perform the following: (1) extract the maximum possible energy from the wind, (2) operate the turbine in safe mode with control variables such as power, voltage, current, speed, and torque under limits, (3) achieve the desired dynamic and steady-state performance, (4) minimize mechanical stress on the drivetrain, and (5) meet strict grid codes (shall be discussed in the next section). The master control system monitors various variables such as wind speed, wind direction, generator voltages/currents, filter/DC-link voltages, and grid voltages/currents. The master control system then adjusts the system operating states or variables at the reference value or in the set boundaries with the support from slave control systems. The control systems are realized by a personal computer, μC, programmable logic controller, DSP, or FPGA. To avoid confusion with mechanical and electrical control systems, in this book, "digital control" is defined as "electrical control" only. The control of WTs is an important subject matter and is discussed further in Section 1.7.

1.4 GRID CODE REQUIREMENTS FOR HIGH-POWER WECS

The steady growth in the power levels of WTs and wind farms have led to the significant penetration of wind energy systems into the existing electric power system. To ensure grid stability and consumer power quality, many specific technical requirements (documents) often called "grid codes" have been developed and are regularly updated by transmission system operators (TSOs) and/or distribution system operators (DSOs) in many countries [27]. The main elements in grid codes include the following:

- Grid voltage and frequency tolerance
- Active power control
- Reactive power generation (RPG)
- Grid power quality
- Black start and short-circuit capability
- Fault ride-through (FRT)

The above requirements stipulate that a wind power plant is expected to act like an active power generation unit, similar to conventional power plants during normal and abnormal grid conditions. The first requirement indicates that WECS must remain operational when the grid voltage and frequency varies within the set boundaries or tolerance band limits. WECS must control the active power output (by disconnecting some WTs from the grid or by pitch control action) according to the power command given by the TSO/DSO, such that active power curtailment and frequency regulation at the PCC is achieved. Some countries also define active power control with respect to the grid frequency variation. For example, according to Danish grid code, when the frequency increases above 48.7 or 50.15 Hz, active power should be decreased depending on the power reserving strategy [5].

WECS must also be able to control reactive power such that the voltage and PF at the PCC is tightly regulated. The RPG requirement must be fulfilled by WECS independent of the type of WT technology being used. In case the WTs cannot produce the required reactive power, additional static compensation devices such as static VAR compensator (SVC) or static synchronous compensator (STATCOM) should be employed in the wind farm. WECS should also provide reactive power during abnormal conditions to support the grid and assist the fast recovery of grid voltage.

Power quality determines the fitness of the electric power to the utility grid. Power quality involves various items such as transient variations, flickers, and harmonics. According to IEEE 519-1992, for voltages below 69 kV, the maximum total harmonic distortion (THD) of the grid voltage at the PCC must be limited to 5% during normal operations to prevent harm to other electrical equipment connected to the utility grid. For voltages in the range of 69 kV to 161 kV, the maximum voltage THD and individual voltage harmonics should be limited to 2.5% and 1.5%, respectively. For voltages above 161 kV, total and individual voltage distortion should not exceed 1.5% and 1%, respectively. Similarly, harmonic current limits are imposed in terms of total demand distortion (TDD) on the basis of the ratio of the three-phase fault current to maximum demand current, I_{sc}/I_L.

Black-start capability indicates the ability of the power generation unit to restore normal operations from shutdown mode without using an external power network. Short-circuit capability indicates the ability of an electrical apparatus to interrupt without being destroyed or causing an electric arc. FRT indicates the ability of WECS to operate through periods of low or high grid voltage. Among all the grid codes, the FRT and RPG are major concerns for WT and power converter manufacturers.

1.4.1 Fault Ride-Through

Grid disturbances such as grid voltage sags/swells might lead to disconnection of large-scale wind power generation units. The sudden disconnection of generation units stimulates the instability of the utility network. Beginning in early 2003, the German utility operator E.ON imposed FRT requirements to overcome the aforementioned scenario [28]. The TSO and DSO of diverse countries issued similar FRT profiles with different grid voltage dip magnitudes and grid fault durations [29]. The FRT requirement is a broad category covering zero-voltage ride-through (ZVRT), low-voltage ride-through (LVRT), and high-voltage ride-through (HVRT). The ZVRT and LVRT requirements correspond to grid voltage sags: during grid faults, the grid voltage becomes zero in the ZVRT profile; in the LVRT profile, the grid voltage becomes 15–25% of its nominal value. The HVRT corresponds to grid voltage swells.

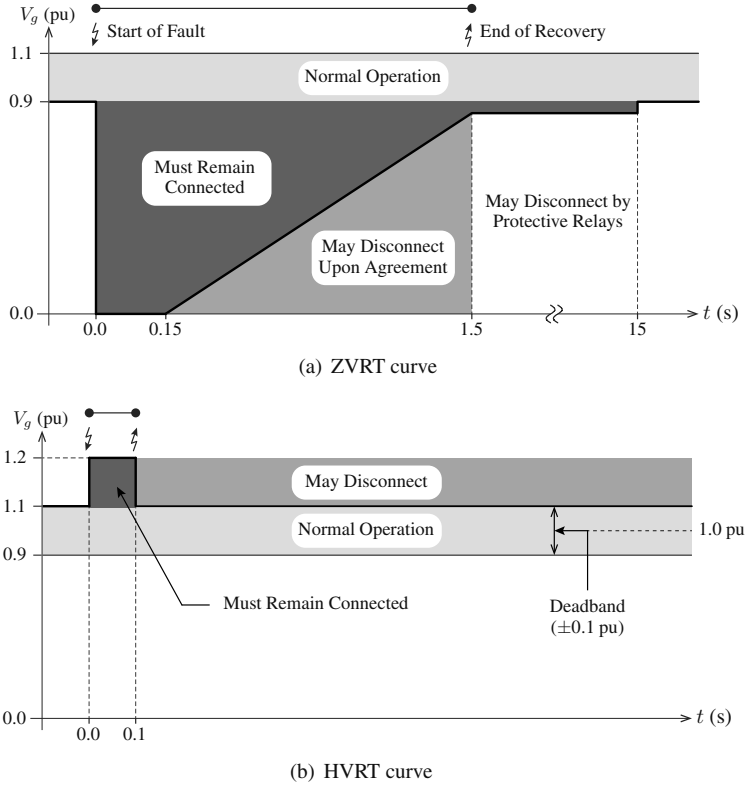

Figure 1.13 FRT requirement according to the E.ON regulation [28].

The ZVRT and HVRT profiles of the E.ON regulation are shown in Figure 1.13. These profiles specify that the WTs must "ride through" instead of "trip off" during transmission faults. During grid voltage sags (refer to Figure 1.13(a)), the FRT function should start within 20 ms (one cycle) when the grid voltage falls below 0.9 pu and should provide 1.0-pu reactive power. The WT must be connected to an electric network if the grid voltage profile is above the ZVRT limit line. The turbine is allowed to disconnect from the grid if the magnitude of the grid voltage falls below the ZVRT limit line. For offshore wind farms, the ± 0.1-pu deadband is reduced to ± 0.05 pu.

During grid voltage swells (see Figure 1.13(b)), when the grid voltage swells to 1.2 pu, the WECS must ride through for 0.1 s. To ensure grid voltage recovery, WECS should absorb 1.0 pu reactive power (opposite to LVRT requirement). Recently, considerable research has been conducted to address the FRT issue in WECS [1, 27].

1.4.2 Reactive Power Generation

In addition to the FRT operation, another important requirement for WECS is that it should perform "reactive power control" similar to a conventional power plant during both normal and abnormal operations. Reactive power control helps compensate transmission equipment such as cables and transformers, in addition to maintaining voltage stability. Thus, reactive power control is an important grid code regulation to maintain reliable and efficient transmission and distribution grids.

Similar to FRT profiles, many reactive power profiles are defined by diverse TSOs and DSOs with respect to the active power output and grid voltage magnitude [30]. The reactive power Q_g requirement as a function of the active power P_g and grid voltage V_g is shown in Figures 1.14(a) and 1.14(b), respectively. PQ dependence according to the German grid code shows the range of Q_g to be delivered by WT GSC with respect to P_g. When WECS delivers rated (1.0 pu) active power, it should be able to supply 0.41 pu or absorb 0.33 pu reactive power. This case implies that WECS should be able to adjust the grid PF anywhere from 0.93 leading to 0.95 lagging when it delivers rated active power. During reduced (0.2 pu) active power output, the range of the PF varies between 0.44 leading and 0.52 lagging (Figure 1.14(a)). The Q_g requirement is variable when P_g is between 0 and 0.2 pu.

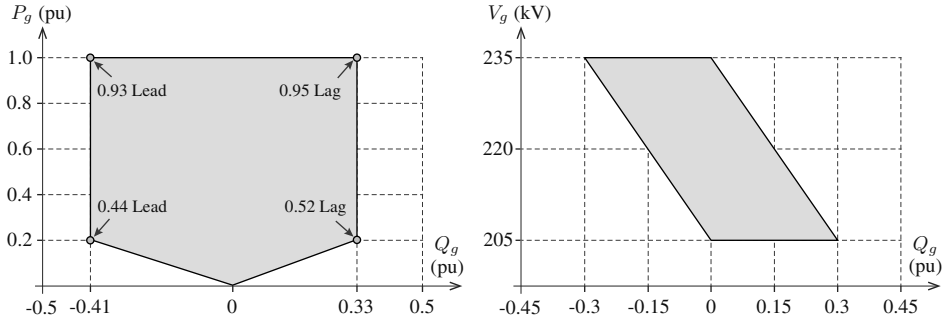

(a) PQ dependence in Germany (b) VQ dependence in Spain

Figure 1.14 Reactive power requirement for grid-connected WECS.

As highlighted in Figure 1.14(b), the VQ dependence curve according to the Spanish grid code shows the Q_g requirement with respect to the grid voltage V_g. In addition to the reactive power requirement during normal operations, WECS must also provide Q_g under the grid faults. For example, according to German and Danish grid codes, WECS must stop injecting active power during grid voltage dips and should generate 1.0 pu reactive power until the grid voltage recovers to 0.5 pu. For grid voltages in the range of 0.5 pu to 0.9 pu, WECS should provide 0.02 pu reactive current for each 0.01 pu grid voltage dip. Although the RPG requirement is a stringent grid code, this requirement can easily be fulfilled by properly designing the following: (1) the WT GSC with high MVA capacity and (2) high-performance digital control for MSC and GSC.

1.5 WECS COMMERCIAL CONFIGURATIONS

The major mechanical and electrical components in WECS are the wind turbine, gearbox, mechanical speed/torque converter, wind generator, power electronic converter, and step-up transformer. By using different designs and combinations with some or all of these mechanical and electrical components, a wide variety of WECS configurations have been commercialized, such as [1, 17, 23, 24]:

- **Type 1:** Fixed-speed WECS with SCIG
- **Type 2:** Semi-variable-speed WECS with WRIG
- **Type 3:** Semi-variable-speed WECS with DFIG
- **Type 4:** Full-variable-speed WECS with SCIG, PMSG, WRSG, or HTS-SG
- **Type 5:** Full-variable-speed WECS with WRSG and mechanical converter

In this section, the above five configurations are analyzed in detail on the basis of Figures 1.15 to 1.19. The major mechanical and electrical components, operating principle, advantages, and disadvantages of each WECS configuration are discussed.

1.5.1 Type 1 WECS Configuration

A fixed-speed SCIG-based WECS without a power converter interface (Type 1 turbine) is illustrated in Figure 1.15, where the generator is connected to the grid through a soft starter and step-up transformer. This technology is the oldest and very first technology ("Danish" concept) developed for WTs during the 1980s [17]. To reduce initial investment and increase reliability, first-generation WTs were developed by using well-proven mechanical and electrical components already existing in the market.

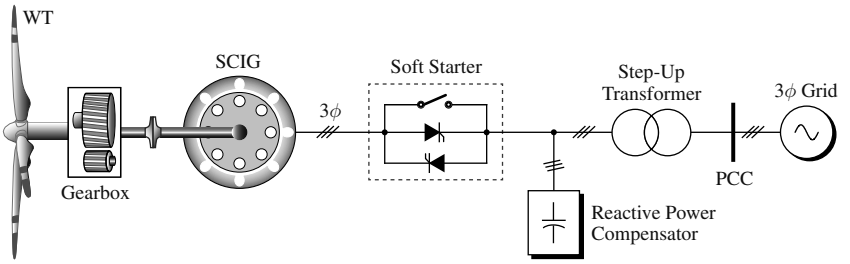

Figure 1.15 Type 1 WECS with fixed-speed (1%) SCIG, three-stage gearbox, soft starter, and reactive power compensator.

In high-power WECS, the SCIG contains four or six poles for 50- or 60-Hz grid frequency operations, respectively. During different wind speeds, the generator speed varies slightly (within 1% above the synchronous speed); hence, this configuration is called fixed-speed WECS. Pole-changeable SCIGs were also practiced in the industry to accomplish two rotational speeds during varying wind speeds. Early WTs employed passive stall aerodynamic power regulation, whereas modern turbines use active stall or pitch control techniques. A three-stage gearbox is normally employed between the turbine rotor and wind generator to match the speed difference between them.

During the startup process, the voltage difference between the wind generator and utility grid causes a high in-rush current. A three-phase soft starter consisting of anti-parallel

thyristors and a bypass switch limits the in-rush current to safe limits. The firing angle of the thyristors is gradually adjusted such that the grid voltage applied to the wind generator changes progressively from zero to the rated value. After the startup procedure, the thyristors are bypassed (because of the limited thermal capacity of the thyristors and to limit power losses) by a switch and the system essentially works without any power converter [13]. The SCIG draws reactive power from the grid; to compensate for this mechanism, three-phase capacitor banks are usually employed. To provide optimal reactive power compensation, multiple capacitor banks are used to switch in and out of the three-phase electric system. Major advantages and disadvantages of this configuration are summarized below:

- ✔ Simple power conversion configuration.
- ✔ Low initial and maintenance costs because of SCIG, and inexpensive soft starter.
- ✔ Reliable operation as no power converter is needed.
- ✖ Lower wind energy conversion efficiency because of narrow (1%) speed range.
- ✖ Changes in wind speed cause grid frequency stabilization issues.
- ✖ Grid faults cause severe stress on the mechanical components of the WT [31].

FSWTs are equipped with additional hardware, such as STATCOM, to comply with the grid codes [32]. Despite the drawbacks, this configuration has been accepted by the wind industry and commercial solutions are available in MW range such as: (1) `Vestas` V82 (1.65 MW) and (2) `Siemens` SWT 2.3-101 (2.3 MW). Fixed-speed turbines were famous until a decade back, but this technology is slowly becoming obsolete because of its inherent disadvantages. The turbines in the present study, which have been installed already, are still in operation to generate electricity.

1.5.2 Type 2 WECS Configuration

To overcome the drawbacks associated with Type 1 WTs, the wind energy industry developed semi-variable-speed WTs. The configuration of a semi-variable-speed WECS using WRIG and a partial rated (10%) power converter is shown in Figure 1.16 (Type 2 turbine). The system configuration is similar to a Type 1 turbine; however, the SCIG is replaced by a WRIG with rotor windings connected to the converter-controlled external resistor. The power converter is realized by a three-phase diode-bridge rectifier and an insulated gate bipolar transistor (IGBT)-based chopper circuit .

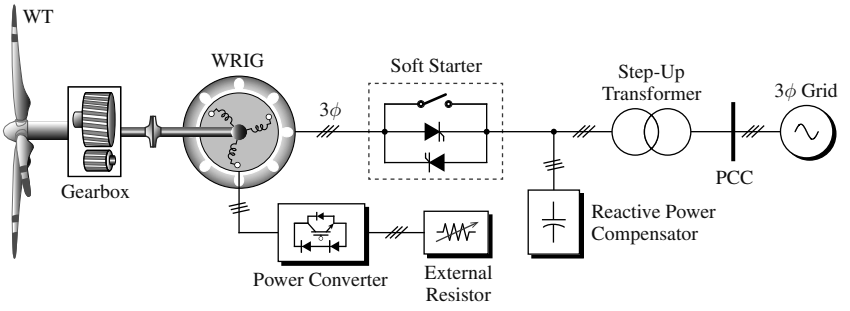

Figure 1.16 Type 2 WECS with semi-variable-speed (10%) WRIG, converter-controlled external resistor, three-stage gearbox, soft starter, and reactive power compensator.

The change in the rotor resistance affects the torque/speed characteristic of the generator, thus enabling the variable-speed operation of the turbine; this configuration is often called Optislip WT [17]. Speed adjustment range is typically limited to approximately 10% above the synchronous speed. With semi-variable-speed operations, WECS can capture slightly higher power from the wind with reduced stress on mechanical components but with energy losses in rotor resistance. This Type 2 configuration also requires a gearbox, soft starter, and reactive power compensation similar to a Type 1 turbine. The main merits and demerits of this configuration are given as follows:

- ✔ Higher energy conversion efficiency than Type 1 turbines because of extended (10%) speed range.
- ✔ Lower stress on WT mechanical components compared with Type 1 turbines.
- ✔ Less effect on grid frequency because of semi-variable-speed operation.
- ✖ Higher initial cost because of the power converter and higher maintenance cost due to slip rings and brushes in WRIG.
- ✖ The external resistor causes system losses and lower reliability.
- ✖ The system still requires soft starter and grid-side reactive power compensation.

The WRIG with variable rotor resistance has been on the market since the mid-1990s with a power rating up to a couple of MWs. A few examples of commercial solutions are as follows: (1) `Vestas` V66-2.0 MW and (2) `Suzlon Energy` S88-2.1 MW. This configuration is also becoming less important among WT manufacturers because of its limited speed range and low energy conversion efficiency.

1.5.3 Type 3 WECS Configuration

In a continued effort to increase the operational speed range of WTs and eliminate soft starter and grid-side reactive power compensator, Type 3 semi-variable-speed turbines were developed. The configuration of Type 3 WECS using a DFIG and power electronic converter is shown in Figure 1.17 [33]. This configuration replaces the converter-controlled external resistor in a Type 2 turbine by a power converter. As the name implies, power from the doubly fed induction generator is fed to the grid through both stator and rotor windings.

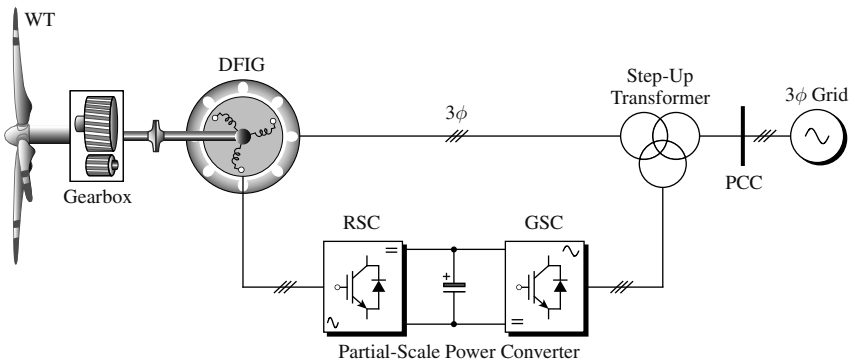

Figure 1.17 Type 3 WECS with semi-variable-speed (±30%) DFIG, three-stage gearbox, and partial-scale (30%) power converter.

The converter in the rotor circuit has to handle only the slip power; thus, the power capacity of this converter should be only 30% of the generator rated power [34]. The use of a partial scale (30%) converter leads to a reduction in cost, weight, and nacelle space requirement. From a cost point of view, a smaller converter capacity makes Type 3 WECS more attractive and popular. The cost of converter in a REPower (now Senvion) MM92-5.0 MW WT was reported as 5% of the total turbine cost [19]. The power converter is usually made of two-level voltage source converters (VSCs) connected in a BTB configuration. The machine-side VSC, also called a rotor-side converter (RSC), controls the generator torque/speed or active/reactive power, whereas the GSC controls the net DC-bus voltage. The power converter is also equipped with harmonic filters on the rotor-side and grid-side to attenuate switching harmonics. The step-up transformer uses three winding structures with two primary windings on the generator side and one secondary winding on the grid side. The main features of Type 3 WECS are summarized below:

- ✔ The power converters allows bidirectional power flow in the rotor circuit. The generator speed is adjustable 30% above or below the synchronous speed. Therefore, the energy conversion efficiency is high and stress on the mechanical components is low.
- ✔ The power converter performs smooth grid connection and grid-side reactive power compensation. Therefore, soft starters and capacitor banks are not needed.
- ✔ The power converter also provides enhanced dynamic performance and robustness against power system disturbances compared with Type 1 and 2 turbines [35].
- ✖ The initial cost and system complexity is high because of the power converter.
- ✖ Unsuitable for offshore wind farms because of the regular maintenance needed by the slip rings and brushes in DFIG and the three-stage gearbox.
- ✖ FRT compliance is complicated because of the direct grid-connected DFIG stator terminals and partial (30%) rated power converter.

Despite the above drawbacks, Type 3 WECS are one of the dominating technologies in today's wind energy industry with a market share of about 50% [36]. Some examples of high-power Type 3 turbines are: (1) REpower (now Senvion) 6M (6.0 MW), (2) Bard 5.0 (5.0 MW), and (3) Acconica AW-100/3000 (3.0 MW).

1.5.4 Type 4 WECS Configuration

To achieve variable-speed operations over the entire wind-speed range, Type 4 turbines were developed during the 1990s. The configuration of Type 4 WECS with a wind generator, and a full-scale power converter composed of machine (generator)-side converter (MSC), DC-link capacitor and GSC is shown in Figure 1.18 [1, 24]. In contrast to Type 3 turbines, where the power converter is connected in the rotor circuit to process slip power, Type 4 turbines employ a power converter between the wind generator stator terminals and utility grid to process all the electric power produced. Therefore, the capacity of the power converter increases from 30% to 100%. The cost of a power converter in Type 3 and 4 WECS is approximately 5% and 7–12% (according to the type of converter topology) of the total WT cost, respectively [19, 37]. A full-scale (100%) power converter leads to full-variable-speed range (0% to 100%) and the energy yield in these turbines is the highest. SCIG, PMSG, WRSG, and HTS-SG have all found applications in this type of configuration with power ratings of up to several megawatts. Among the classes of wind generators, PMSG is the most popular in Type 4 WECS (refer to Table 1.2 on page 20 for advantages of PMSG over other wind generators).

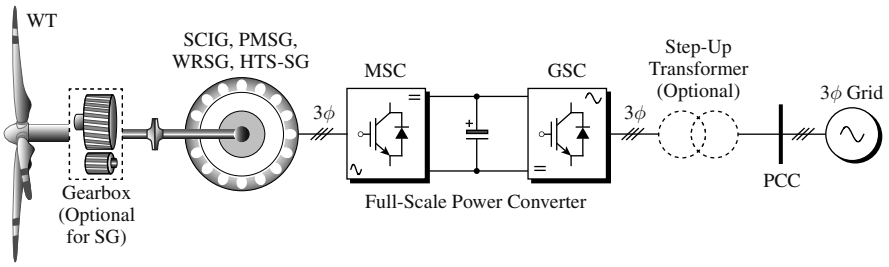

Figure 1.18 Configuration of Type 4 WECS with full-variable speed (0 – 100%) wind generators, optional gearbox, and full-scale power converter.

The BTB connected power converter configuration shown in Figure 1.18 is similar to the one shown in Figure 1.17 in terms of construction, modulation, and digital control. This power converter can provide or consume reactive power; thus, it represents dynamic capacitor/inductor bank and helps maintain power system stability. The step-up transformer can be eliminated by operating the power converters at a MV level. The significant pros and cons of this configuration are as follows:

✔ High-energy yield and no stress on mechanical components because of full-variable-speed (0 – 100%) operation.

✔ Independent active and reactive power control lead to excellent FRT compliance.

✔ The generator is fully decoupled from the grid. The power converters also enable smooth grid connection.

✖ Owing to the full-scale converter, the initial cost and nacelle space requirement increase along with overall system complexity.

✖ Higher power losses in the converter degrade overall efficiency.

✖ The complexity of digital control system design for power converters increases.

Wind energy conversion efficiency in Type 4 WECS is the highest compared with other types of turbines. The high-energy yield compensates the drawbacks of high converter cost and power losses. The need for the gearbox can be eliminated by using a high-pole number SG. This configuration is more robust against power system faults than Type 1, 2, and 3 turbines [38]. The best FRT compliance is achieved by a full-scale converter and an external static reactive power compensator is not needed. Typical commercial turbines include: (1) `Enercon` E126 (7.5 MW), (2) `Multibrid` M5000 (5.0 MW), and (3) `Vestas` V-112 (3.0 MW).

The distributed drivetrain concept is used in recent megawatt Type 4 WTs with a PMSG to obtain a simple design. The gearbox drives multiple generators at high speeds. The distributed drivetrain and multiple generators enable the achievement of high power density [39]. One commercial application is `Clipper Liberty` C99 WT, which uses a quantum drivetrain, four PMSGs, and four converters. The high torque is distributed among the four drivetrains, and the power rating of the converters is one-fourth of the system rating. This configuration also offers an effective fault-tolerant operation. When one converter fails, the other three converters can still deliver the power to the grid. The main disadvantage of using this configuration is the complicated drivetrain.

1.5.5 Type 5 WECS Configuration

The Type 5 WT with a direct grid-connected WRSG (EESG), two-stage helical/planetary gearbox, and mechanical speed/torque converter is shown in Figure 1.19. This configuration, wherein the variable-speed operation is achieved by a mechanical converter rather than an electrical converter, is an old concept for WTs. The torque/speed converter, also known as a variable ratio transmission, converts the variable speed of the WT to a constant speed. The generator operates at a fixed speed and is directly connected to the grid through a synchronizing circuit breaker. The rotor in the WRSG carries a field winding to produce rotor flux. The rotor DC excitation current is provided by a small AC/DC power converter that is directly connected to the three-phase grid (low-voltage side of a step-up transformer, if any). The DC excitation also includes slip rings and brushes (or brushless exciter). The excitation current is adjusted such that the generator output voltage and frequency match the grid code requirements. One of the major drawbacks with this configuration is that the field winding losses in WRSG reduce generator efficiency compared with PMSG.

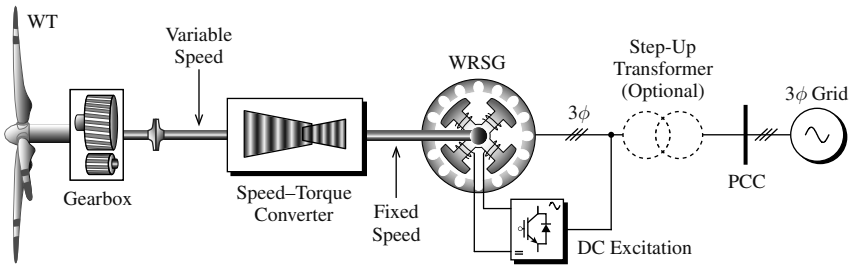

Figure 1.19 Configuration of Type 5 WECS with a fixed-speed WRSG, three-stage gearbox, and steed-torque converter.

The main features of this WECS configuration are summarized as follows:

- ✔ Similar to the Type 4 WECS, wind energy conversion efficiency is high because of the full-variable-speed range (0 – 100%).
- ✔ The overall cost and nacelle space requirement is lower than Type 4 WECS because of the absence of a converter.
- ✔ The generator can be directly connected to the MV collection point without any step-up transformer because there is no restriction imposed by the power electronic converter unlike the Type 4 turbine.
- ✖ The configuration has high system complexity because of the mechanical speed/torque converter.
- ✖ Type 5 WECS is unsuitable for offshore applications because of the high maintenance of the gearbox and mechanical speed/torque converter.
- ✖ The FRT compliance becomes complicated because it must be handled solely by the WRSG excitation system.

Despite the good features of this configuration, it is rarely used in the wind energy industry because of issues related to the mechanical converter. Currently, only three WT manufacturers use this technology: (1) `DeWind` D8.2 (2.2 MW, 4.16/13.8 kV); (2) `Wikov` W2000 (2.0 MW, 6.3/11 kV); (3) `AMSC-Windtec` SuperGear (2.0 MW, 11 kV). These turbines can be directly connected to a medium-voltage distribution line without a step-up transformer because of MV-WRSGs.

1.5.6 Comparison of WECS Configurations

The main features and drawbacks of all five types of wind energy configurations are summarized in Table 1.4. Comparisons and analyses are performed on the generator, power converter configuration, power converter capacity, achievable speed range, soft-starter requirement, gearbox, external reactive power compensator, MPPT ability, aerodynamic power control, compliance with the FRT requirement, technology status, and market penetration. Each configuration has its own merits, demerits, and practical applications.

Table 1.4 Summary of the five types of wind energy system configurations [1]

	Fixed Speed	**Semi-Variable Speed**		**Full-Variable Speed**	
	Type 1 WECS	Type 2 WECS	Type 3 WECS	Type 4 WECS	Type 5 WECS
Generator	SCIG	WRIG	DFIG	SCIG, SG ①	WRSG
Speed Range	1%	10%	±30%	0 – 100%	0 – 100%
Power Converter	Not Required	Diode+Chopper	AC/DC+DC/AC ②	AC/DC+DC/AC ②	Not Required
Converter Capacity	0%	10%	30%	100%	0%
Soft Starter	Required	Required	Not Required	Not Required	Not Required
Gearbox	3–Stage	3–Stage	3–Stage	3/2/1/0–Stage ③	2–Stage
Reactive Power Compensation	Required (Capacitors)	Required (Capacitors)	Not Required	Not Required	Not Required
Aerodynamic Power Control	Active Stall, Stall, Pitch	Pitch	Pitch	Pitch	Pitch
MPPT Operation	Not Possible	Limited	Achievable	Achievable	Unknown
FRT Compliance	By External Hardware	By External Hardware	By Power Converter	By Power Converter	Unknown
Technology Status	Outdated	Outdated	Highly Mature	Mature/Emerging	Old Concept
Current Market Penetration	Few or No Installations	Few or No Installations	Highest Share (>50 %)	2nd Highest Share ④	Few Installations
Example WTs	Vestas V82 1.65 MW	Suzlon S88 2.1 MW	REpower 6M 6.0 MW	Enercon E-126 7.5 MW	DeWind D82 2.2 MW

① SG includes PMSG, WRSG, and HTS-SG
② Direct AC/AC conversion is also possible without an intermediate DC stage
③ Three-stage gearbox is mandatory with the SCIG
④ PMSG is the most favored industry choice in this category

To demonstrate the popularity of each WECS configuration in the wind energy industry, the top 10 WT manufacturers in 2014 and their priority generator and gearbox technologies are illustrated in Figure 1.20. These manufacturers account for approximately 72% of the 51.5 GWs installed wind power capacity in 2014 [4]. The Danish company Vestas remained on the top of the list with a 12.3% share from both onshore and offshore installations. WT manufacturers Siemens, GE Energy, Goldwind, Enercon, Suzlon Group, United Power, Gamesa, Ming Yang, and Envision hold the top 2 to 10 positions in order. Four Chinese companies belong to the top 10 manufacturers list with a cumulative market share of 22.3%.

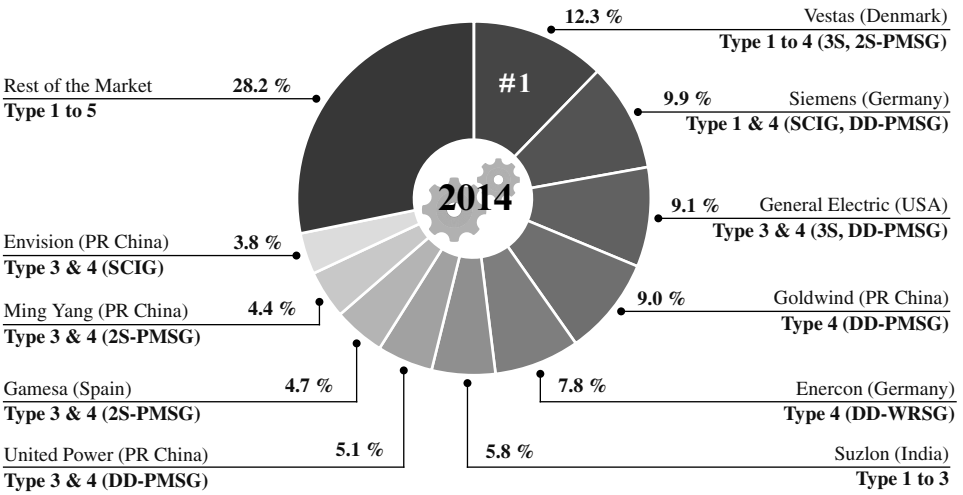

Figure 1.20 Top 10 WT manufacturers in 2014, along with their priority WECS configurations.

The WECS configuration, wind generator, and gearbox employed by the top 10 WT manufacturers are also shown in Figure 1.20. These details are obtained from the product brochures of the companies. Type 3 turbines (DFIG), which have the highest market share, are used by 7 of the top 10 manufacturers. Approximately 100 different DFIG turbine models are offered by the WT manufacturers. Type 4 turbines are produced by 6 manufacturers, and 4 of these manufacturers offer direct-drive solutions. The best-selling WTs in the market use Type 3 and 4 technologies. Future project announcements from WT manufacturers indicate that Type 4 technology will take over the market in the coming years. This book deals with Type 3 and 4 turbines only.

1.6 POWER ELECTRONICS IN WIND ENERGY SYSTEMS

The analysis of all five types of WECS configurations in the previous section indicates that since the production of the first-generation fixed-speed WTs in the 1980s, power electronics technology has an important collaboration with the grid-connected WTs. The power electronics technology contributes to low cost of energy, extraction of maximum possible energy from wind, enhancement of reliability and power density, fault-tolerant operation, reduction of weight and footprint, superior grid power quality, compliance with the strict grid codes, etc. Examples of the applications of power electronics in WECS are as follows:

- As a soft starter for a smooth grid connection (limiting startup in-rush currents) of Types 1 and 2 turbines.
- As a power converter to adjust rotor circuit resistance value and the slip characteristics of WRIG in Type 2 turbines.
- As a partial-scale converter to handle the slip power of DFIG and to increase speed range in Type 3 turbines.
- As a full-scale converter to decouple the generator from the grid and provide a full-speed range in Type 4 turbines.
- As an AC/DC converter to adjust the excitation current for WRSG in Type 5 turbines such that the generator output voltage and frequency matches the grid conditions

Power electronics technology has undergone considerable advancement, and state-of-the-art solutions are available in the form of full-scale high-power converters. Current technology uses power electronics in WTs and WFs for energy conversion and grid integration. Power converters facilitate variable-speed operation in Type 3 and 4 WECS while eliminating the need for a soft starter and reactive power compensation. To enable the grid connection of these WTs, the variable voltage/frequency of the wind generator should be converted into a fixed voltage/frequency. Thus, a wide variety of power conversion stages can be employed as highlighted in Figure 1.21 [8]. Most power conversion stages have found commercial applications, and some have been proposed in literature with promising features for future development, whereas other topologies have been derived from the variable-speed electric drives industry. Converters are broadly classified as direct and indirect: direct conversion uses single-stage AC/AC power converters, whereas indirect conversion uses two-stage (AC/DC + DC/AC) or three-stage (AC/DC + DC/DC + DC/AC) power converters. The direct and indirect power converters in Figure 1.21 are further classified into LV and MV category.

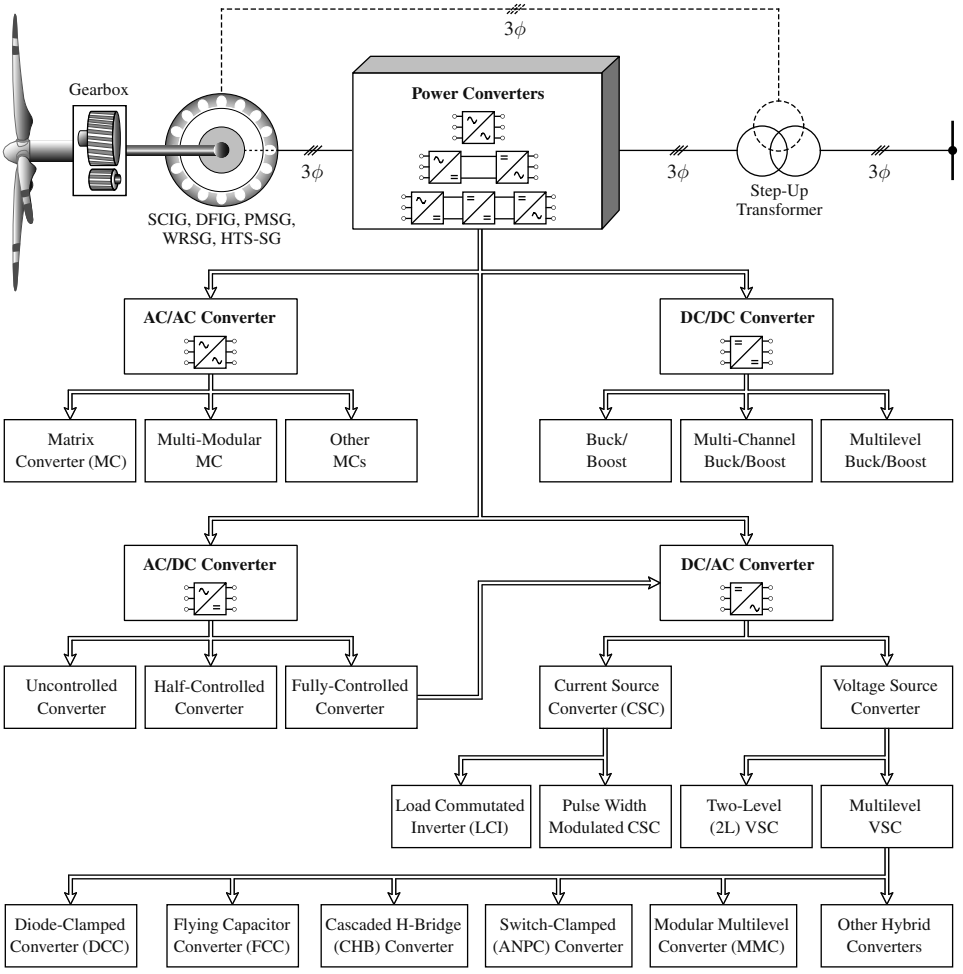

Figure 1.21 Taxonomy of power converters for Type 3 and 4 variable-speed WECS.

Direct AC/AC (matrix) converters compete with two-stage (AC/DC + DC/AC) VSCs in the electric drives industry because of the elimination of DC-link components and high reliability. The AC/AC converters are available in the form of direct and indirect MCs in the LV category or as multi-modular MC in the MV category. Although MCs have not been used in the WECS industry, Yaskawa, a leading matrix converter manufacturer, has developed an MV matrix converter product (Enewin-MX1) for high-power WTs [40].

Indirect two-stage (AC/DC + DC/AC) power converters are widely available in a BTB connected configuration. A fully controlled AC/DC converter, DC-link components such as capacitors and inductors, and a DC/AC converter form the BTB configuration. BTB converters are used as VSCs and CSCs. In the WECS industry, BTB VSCs are well proven, low cost, and reliable. These converters facilitate (inherently) a four-quadrant operation with a relatively simple configuration. Furthermore, BTB VSCs are suitable for both Types 3 and 4 WECS with IGs and SGs. The BTB 2L-VSC and parallel 2L-VSCs are used in the LV category. For high-power WTs, MV converters are preferred. The three-level DCC or neutral-point-clamped (NPC) converter topology is the most attractive choice in the wind energy industry. This topology increases the output voltage without connecting switching devices in series (i.e., no derating), reduces *dv/dt* stress compared with 2L-VSC, minimizes the harmonic filter requirement, and improves the grid power quality. The neutral-point voltage control is a challenging issue and has been extensively researched in literature. MV converters such as FCC, CHB converter, ANPC converter, and PWM CSC are popular in the electric drives industry [41] and are promising for future developments in the WECS industry. MMC is a recent development for HVDC applications, and many current research works study its suitability for the WECS industry.

Indirect three-stage (AC/DC + DC/DC + DC/AC) power converters are also employed by a few WT manufacturers. The generator-side AC/DC conversion is performed by an uncontrolled converter (diode-bridge rectifier). Diode rectifiers are cheap and reliable compared with IGBTs. Intermediate DC/DC converters perform variable-speed operations for WECS. The DC/AC converter is similar to the one employed in two-stage converters. Three-stage power converters are only suitable for Type 4 WECS with SGs because the power flow is unidirectional (from the generator to the grid).

1.7 CONTROL OF WIND ENERGY SYSTEMS

Control theory has evolved as an important discipline in modern WTs and WFs. Control schemes enforce WECS to achieve the desired operation, increase wind energy conversion efficiency, reduce energy cost, increase the lifespan of WT components, decrease structural loading, decrease turbine down times, and provide a superior dynamic and steady-state performance. In this section, the control of mechanical and electrical power conversion units are discussed in detail.

The block diagram of the overall control scheme for a modern variable-speed WECS is shown in Figure 1.22. The analysis given in this section is applicable for Type 3 and 4 WECS. The stator and rotor connections of Type 3 DFIG WECS are shown by the dotted lines. The power conversion system in Type 3 and 4 WECS is realized by RSC + GSC and MSC + GSC, respectively. The WECS mainly consists of six control levels, wherein the Level I control loop involves fast varying variables and the Level VI control loop comprises by slow-varying variables. The tight control of variables in Level I loop is important to fulfill the active and reactive power commands imposed by the TSO/DSO in the Level VI control loop. The control loops also consider normal and abnormal operation for WECS.

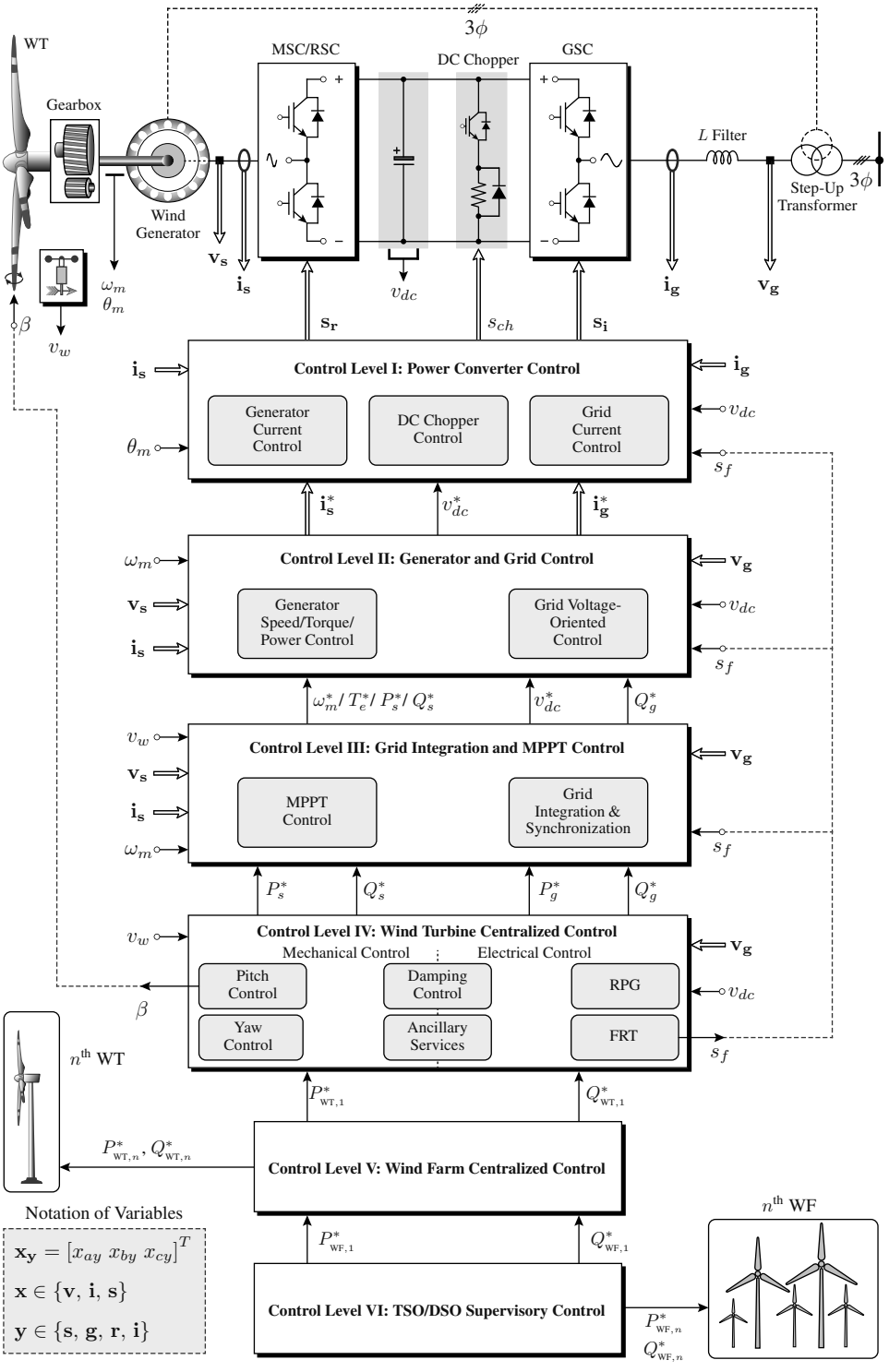

Figure 1.22 Block diagram of the overall control scheme for variable-speed WECS [5, 30, 42].

During grid faults, the FRT control in the Level IV loop issues a fault enable signal s_f. The mechanical and electrical control systems in the Level I to IV loops coordinate for better control performance during grid faults. For example, during grid faults, the GSC stops injecting active power and produces reactive power to the grid, the pitch control system starts working to decrease power extraction, and the DC chopper starts functioning to prevent the DC-bus voltage from exceeding the upper threshold limit.

The feedback signals from the WECS such as grid voltages $\mathbf{v_g}$, grid currents $\mathbf{i_g}$, generator voltages $\mathbf{v_s}$, generator currents $\mathbf{i_s}$, DC-link voltage v_{dc}, generator angular speed ω_m, rotor position angle θ_m, and wind speed v_w are used by various control loops. For DFIG WECS, the rotor currents are measured additionally. The control requirements are met by generating optimal gating signals $\mathbf{s_r}$, $\mathbf{s_i}$, and s_{ch} for the MSC/RSC, GSC, and DC chopper, respectively. The three-phase variables are represented by an equivalent vector, for example, $\mathbf{x_y} = [x_{ay}\ x_{by}\ x_{cy}]^T$. The main variable $\mathbf{x}$ denotes the voltage, current, or switching signal ($\mathbf{x} \in \{\mathbf{v},\ \mathbf{i},\ \mathbf{s}\}$). The subscript $\mathbf{y}$ represents the source (generator), grid, rectifier, or inverter ($\mathbf{y} \in \{\mathbf{s},\ \mathbf{g},\ \mathbf{r},\ \mathbf{i}\}$). The vector variables are denoted by a double line arrow ($\Rightarrow$), and the scalar variables are represented by a single line arrow ($\rightarrow$).

1.7.1 TSO/DSO Supervisory Control (Level VI)

The power output from the WT or WF is highly variable depending on wind-speed conditions. The variable energy in the existing energy mix brought serious reliability and security issues because of the intensive penetration of large-scale WECS into the existing power system. With the efforts made by the TSOs and DSOs through strict grid codes, large-scale wind farms changed their operations over the years from being passive power generation sources to active generation units with grid support characteristics.

Large-scale wind farms are connected to the TSO/DSO dispatch centers through communication networks to continuously share information about active and reactive power generation statuses. The top-level TSO/DSO supervisory control (Level VI) sends active and reactive power commands to each wind farm (similar to conventional power plants) connected to the power system. The first wind farm receives $P^*_{\text{WF},1}$ and $Q^*_{\text{WF},1}$, and the n^{th} wind farm receives $P^*_{\text{WF},n}$ and $P^*_{\text{WF},n}$ commands from TSO/DSO [42]. To simplify the diagram, the communication link and measurements from the wind farm to the TSO/DSO supervisory control are not shown.

1.7.2 Wind Farm Centralized Control (Level V)

The power commands from the Level VI control is received from the WF centralized control. The WTs are connected to the WF centralized control by communication links to share the active and reactive power generation statuses. The supervisory control and data acquisition system is used for WF monitoring. The WF centralized control defines the active and reactive power requirements for each WT. The first WT is commanded with $P^*_{\text{WT},1}$ and $Q^*_{\text{WT},1}$, and the n^{th} WT is supplied with the $P^*_{\text{WT},n}$ and $Q^*_{\text{WT},n}$ commands. The active and reactive power references are calculated such that the frequency and voltage at the PCC are maintained at the desired values. If the WF centralized control learns that the WTs cannot meet the RPG requirement, the wind farm static compensators such as STATCOM or SVC are initiated to support the WTs. The WF centralized control takes every possible effort to command the WTs such that the P and Q references imposed by the superior Level VI control loop are met all the time. The aerodynamic interaction of the WTs is also surpassed by the WF centralized control [43].

1.7.3 WT Centralized Control (Level IV)

As shown in Figure 1.22, the WT centralized control includes both mechanical and electrical controls. The pitch control and yaw control is solely involved in mechanical control, whereas RPG and FRT correspond to electrical control. The damping control includes both mechanical and electrical aspects: mechanical damping control lessens the mechanical resonances in the tower and torsional vibrations in the drivetrain, whereas electrical damping control provides damping for electrical subsynchronous resonances in the grid. The electrical ancillary services include electrical energy storage, uninterruptible power supply (UPS), and power quality. The UPS unit with battery energy storage forms an emergency power supply backup for pitch and yaw drives. Inertia emulation, spinning reserve, and kinetic energy storage are included in mechanical ancillary services [30].

The grid voltage magnitude is continuously monitored by the FRT subsystem. When the grid voltage falls below or above the preset magnitude, it sends a fault enable signal, s_f. This fault signal is sent to the other control loops and other functions inside the Level IV control loop. By coordinating various mechanical and electrical control systems, the WT centralized control provides active power reference P_s^* for WT MSC (P_s^* and reactive power reference Q_s^* for RSC), along with P_g^* and Q_g^* to the GSC. During normal grid conditions, Q_g^* is set to zero to maintain unity grid PF in Type 4 WECS. In DFIG WECS, grid PF is adjusted through Q_s^* command while setting Q_g^* to zero.

As mentioned in Section 1.2.3, modern variable-speed WTs use a pitch mechanism to change the rotation of blades in their longitudinal axis. Three individual electric pitch drives are commonly used in current WTs. The block diagram of the pitch control system is illustrated in Figure 1.23(a). When the wind speed is lower than the rated value, the pitch angle β is kept constant at zero degrees to extract the maximum possible energy from the wind. When the wind speed is higher than the rated value, the proportional-integral (PI) controller produces β such that the generator output power is limited to its rated value. As shown in Figure 1.23(b), as pitch angle increases, C_p decreases along with the extracted wind power (refer to Equation (1.2)), and the generator power comes back to the nominal value. In practice, the pitch control system is realized by a high-performance μC, generator output voltage and current sensors, three DC/AC power converters, three electric motors, and a backup power supply. The μC generates gating signals for power converters on the basis of wind-speed data, measured generator output power, preset power rating, and so on. Power converters change the speed of the three independent electric motors according to the instructions given by the μC.

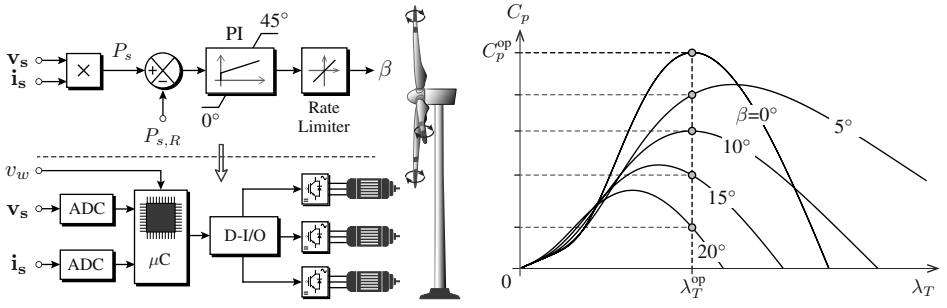

(a) Block diagram and implementation

(b) C_p versus λ_T curve with different β values

Figure 1.23 Pitch control system for high-power WTs (D-I/O: digital input/output).

To show the importance of pitch control in WECS, the turbine characteristics during high-wind-speed conditions is plotted without and with pitch control in Figures 1.24(a) and 1.24(b), respectively. In both cases, the wind speed v_w is assumed to change in a trapezoidal manner with minimum and maximum speed velocities of 1.0 and 1.25 pu, respectively. In the first illustration in Figure 1.24(a), the pitch control is deactivated (β = 0°). As a result, the generator P_s changes in a trapezoidal manner with 1.0 and 1.95 pu as minimum and maximum values, respectively. By neglecting losses, P_s maintains a cubic relationship with respect to v_w. The corresponding generator output current magnitude increases significantly. This result leads to generator and power cable insulation damage and the cascaded failure of the whole WT with possible fire in the nacelle. In the second case, as illustrated in Figure 1.24(b), the pitch angle is adjusted dynamically by the PI controller as wind speed changes; thus, the generator output power and currents are maintained at a rated value. This leads to a safe WT operation with less stress on the electrical and mechanical structural components.

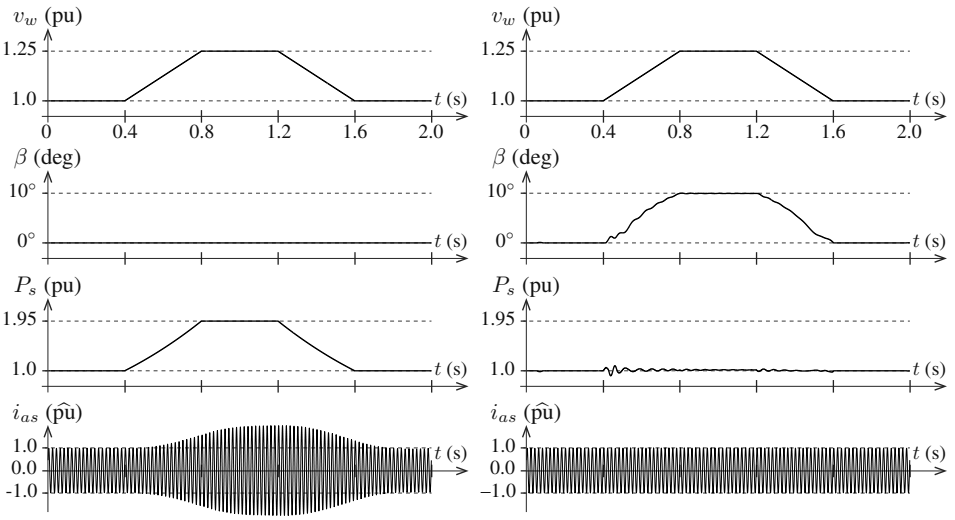

(a) Without pitch control (b) With pitch control

Figure 1.24 Analysis of wind energy system without and with pitch control system.

1.7.4 Grid Integration and MPPT Control (Level III)

The Level III control loop includes the peak power extraction, also called MPPT, grid integration, and synchronization. By employing a grid synchronization algorithm, the phase angle between grid currents and grid voltages can be adjusted accurately with the grid PF requirement. Grid synchronization is performed by zero-crossing detection, grid voltage filtering, or phase-locked loop (PLL). The latter is preferred because of its robustness against grid voltage harmonics and digital control platform friendliness [30]. The control system for a GSC helps in grid synchronization and integration by employing a PLL. The output of the grid integration subsystem is the reference DC-bus voltage v_{dc}^* and reference grid reactive power Q_g^*. For a given grid voltage magnitude v_{dc}^* is usually set constant according to the required modulation index of a GSC.

With the random nature of wind speed v_w, the peak power extraction is important in variable-speed WECS because it increases energy conversion efficiency. For a given v_w value, the MPPT control attempts to obtain the maximum possible power from the wind. As shown in Figure 1.25(a), the maximum power point (MPP) trajectory changes with respect to the wind speed. According to this curve, the operating region for the MPPT control is the cut-in wind speed to the rated wind speed. To facilitate the discussion of various MPPT control techniques, the notation and correlation of variables for a variable-speed WT is shown in Figure 1.25(b).

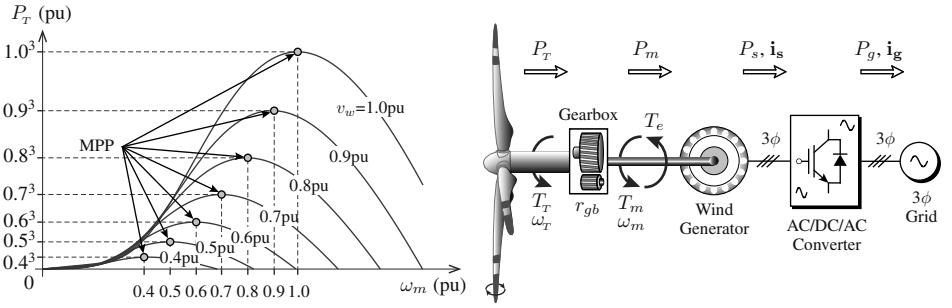

(a) P_T versus ω_m curve (b) Notation of variables in VSWT

Figure 1.25 Power characteristics and notation of variables for VSWT.

The major observations are listed below, assuming that the blade pitch angle is set to its rated (zero) value:

- Turbine output power, mechanical torque, and angular rotational speed are P_T, T_T, and ω_T, respectively.
- Wind generator input power, mechanical input torque, and angular rotational speed are P_m, T_m, and ω_m, respectively. The generator electromagnetic torque is T_e. In a steady-state condition, T_m becomes equal to T_e.
- Wind generator output power and current are P_s and $\mathbf{i_s}$, respectively.
- The power and currents injected to the grid are P_g and $\mathbf{i_g}$, respectively.
- The gear ratio r_{gb} employed in the gearbox increases the generator speed ω_m and decreases the mechanical input torque T_m (i.e., $\omega_m = \omega_T \times r_{gb}$ and $T_m = T_T / r_{gb}$).
- Assuming that no losses occur in the gearbox, drivetrain, and wind generator, the power variables are determined, such that $P_T = P_m = P_s$.
- Turbine and generator speed is proportional to the wind speed because of the variable-speed operation (i.e., $\omega_T \propto v_w$ and $\omega_m \propto v_w$).
- Based on the WT characteristics in Equation (1.2), turbine output power is proportional to cubic of the wind speed (i.e., $P_T \propto v_w^3$). Rotational speed ω_m is proportional to v_w, hence the above notation can be rewritten as $P_T \propto \omega_m^3$.
- Turbine output power is a product of torque and speed (i.e., $P_T = T_T \times \omega_T$). Similarly, for a wind generator, $P_m = T_m \times \omega_m$.
- According to the above representation, the turbine output torque is proportional to the square of the wind or rotor speed (i.e., $T_T \propto v_w^2$ or $T_T \propto \omega_m^2$). A similar expression can be applied to wind generator: $T_m \propto v_w^2$ or $T_m \propto \omega_m^2$.

By utilizing the above notation, various MPPT control techniques, as shown in Figure 1.26, have been developed in literature and applied in the wind energy industry [13, 44, 45]. These techniques determine the reference speed ω_m^*, reference electromagnetic torque T_e^* or reference power P_s^*, such that control Levels I and II force the WECS to follow the MPP trajectory. MPPT control can be achieved by MSC/RSC or GSC, although the most common approach uses MSC/RSC to reduce complexity. MPPT techniques are broadly classified as wind/rotational speed sensor-based methods or speed sensorless (SSL) methods. These methods also vary according to the required input variable (sensor), prior WT knowledge, control complexity, and memory. A brief description of various MPPT control techniques is given below.

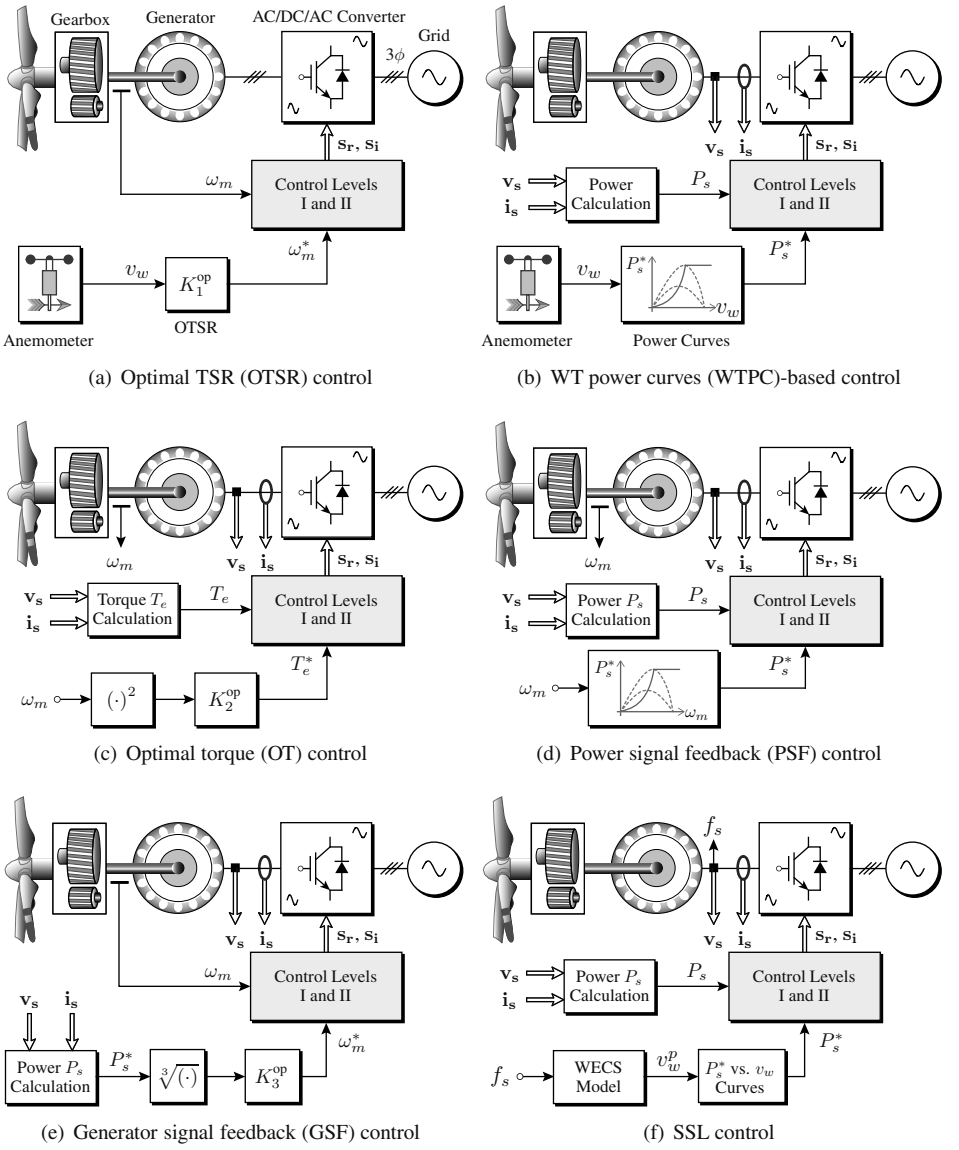

(a) Optimal TSR (OTSR) control

(b) WT power curves (WTPC)-based control

(c) Optimal torque (OT) control

(d) Power signal feedback (PSF) control

(e) Generator signal feedback (GSF) control

(f) SSL control

Figure 1.26 MPPT control of variable-speed wind energy systems.

(1) Optimal Tip Speed Ratio Control: The MPPT with optimal tip speed ratio is shown in Figure 1.26(a). This algorithm provides reference speed ω_m^* on the basis of the measured wind speed v_w and other WT parameters [46]. The generator reference speed ω_m^* is adjusted in proportion to v_w, such that the WT always operates at the λ_T^{op} value to reach the MPP. This adjustment is demonstrated as follows on the basis of the TSR expression given in (1.4):

$$\omega_m^* = \omega_{_T}^* \, r_{gb} = \left(\frac{\lambda_T^{\text{op}} \, r_{gb}}{r_{_T}} \right) v_w = K_1^{\text{op}} \, v_w. \tag{1.5}$$

In the above expression, the gain K_1^{op} can be calculated offline on the basis of the rated turbine parameters. Control Levels I and II use generator feedback speed to minimize the error between ω_m^* and ω_m. This method is the simplest MPPT method among the classes and is widely employed in the WECS industry. By using this approach, no additional memory or prior WT power characteristics knowledge is required. The MPPT control performs well under varying wind speed conditions, because ω_m^* is proportional to the measured v_w. The speed sensor adds cost and complexity to the system. Moreover, obtaining an accurate wind speed is important to ensure that MPP is achieved under different wind speed conditions. Ultrasonic sensors are promising for this control as they provide more accurate and reliable wind-speed information.

(2) WT Power Curves-Based Control: Another wind speed sensor-based MPPT control is shown in Figure 1.26(b). This method uses turbine power $P_{_T}$ versus wind speed v_w curve provided by the WT manufacturer. In initial experimental tests, the generator output power P_s versus wind speed v_w curve can be deducted. By using these WTPCs, the reference power P_s^* is measured at different wind speeds. The MPPT control requires a memory space to store the data points associated with the power curves. Generator output voltages and currents ($\mathbf{v_s}$ and $\mathbf{i_s}$) are measured to compute instantaneous output power P_s. Control Levels I and II generate gating signals for the power converter to minimize the error between P_s^* and P_s. The performance of the WTPC-based control is similar to OTSR control because both mechanisms use wind speed sensors.

(3) Optimal Torque Control: The two MPPT methods mentioned earlier use wind speed sensors that are expensive and do not provide information that is 100% accurate. The MPPT can also be realized by replacing the wind-speed sensor with a generator speed sensor. The operating principle of optimal torque control with a generator speed sensor is shown in Figure 1.26(c), where the measured ω_m is used to compute reference electromagnetic torque T_e^*. On the basis of the TSR expression given in (1.4), the wind speed can be calculated as follows:

$$v_w = \frac{\omega_{_T} \, r_{_T}}{\lambda_T}. \tag{1.6}$$

Substituting Equation (1.6) into (1.2) yields the following:

$$P_{_T} = \frac{1}{2} \, \rho \, \pi \, r_{_T}^2 \, v_w^3 \, C_p = \frac{1}{2} \, \rho \, \pi \, r_{_T}^5 \, \frac{\omega_{_T}^3}{\lambda_T^3} \, C_p. \tag{1.7}$$

The variable-speed WTs operate at optimal TSR λ_T^{op} and optimal power coefficient C_p^{op}. From the notation discussed earlier, we have turbine torque $T_{_T} = P_{_T}/\omega_{_T}$, turbine speed $\omega_{_T} = \omega_m/r_{gb}$, and generator torque $T_m = T_{_T}/r_{gb}$. In a steady state, the generator electromagnetic torque T_e is equal to the mechanical input torque T_m.

Therefore the expression in (1.7) is reorganized as follows:

$$T_e^* = T_m = \frac{T_T}{r_{gb}} = \frac{P_T}{r_{gb}\,\omega_T} = \left(\frac{1}{2}\,\rho\,\pi\,r_T^5\,\frac{C_p^{\text{op}}}{\lambda_T^{\text{op}3}\,r_{gb}^3}\right)\omega_m^2 = K_2^{\text{op}}\,\omega_m^2. \tag{1.8}$$

The coefficient for OT control, K_2^{op} can be calculated offline according to the rated WT parameters. Thus, its control complexity is similar to the OTSR method. In the above expression, the generator mechanical and electromagnetic torque maintains a quadratic relationship with the rotor speed ω_m. Owing to the Levels I and II control, generator electromagnetic torque T_e (and also mechanical input torque T_m) becomes equal to its reference electromagnetic torque T_e^* in a steady state. Similar to the OTSR, the OT control method is also widely used in commercial WTs.

(4) Power Signal Feedback Control: The block diagram of MPPT with the PSF control is shown in Figure 1.26(d) [11]. This approach combines the merits of the WTPC and OT control methods: the wind-speed sensor is replaced by a generator speed sensor and power curves are used to compute reference power P_s^*. As mentioned earlier, in variable-speed turbines, the generator speed varies in proportion to the wind speed (i.e., $\omega_m \propto v_w$); thus, P_s^* versus v_w curves can also be used as P_s^* versus ω_m curves. The PSF control calculates reference power P_s^* based on the measured generator speed ω_m.

(5) Generator Signal Feedback Control: As shown in Figure 1.26(e), the GSF control uses a slightly different concept from PSF control. The computed generator output power P_s is used to calculate reference generator speed ω_m^*. The relationship between P_s and ω_m^* is shown below:

$$\omega_m^* = K_3^{\text{op}}\,\sqrt[3]{P_s}. \tag{1.9}$$

Similar to the OTSR and OT control, the coefficient K_3^{op} for GSF control can be computed offline according to the nameplate parameters.

(6) Speed Sensorless Control: The SSL MPPT control eliminates the need for wind and generator speed sensors. The block diagram of the SSL MPPT control is illustrated in Figure 1.26(f). In this method, autoregressive statistical models of WECS are used to predict wind speed (v_w^p) based on measured generator frequency f_s [47]. Once the wind speed is predicted, reference power P_s^* is calculated similar to WTPC control based on P_s^* versus v_w curves. It is also possible to realize sensorless OTSR control based on the predicted wind speed. This approach eliminates the need for speed sensors; however, it increases the overall complexity of the MPPT control.

(7) Other MPPT Algorithms: MPPT control is a highly researched area in wind energy systems. Many advanced MPPT algorithms based on adaptive control, sliding-mode control (SMC), fuzzy logic control (FLC), artificial neutral networks (ANN), and hybrid combinations have been researched to further increase wind energy conversion efficiency [44]. The perturb and observe (P&O), also called hill-climb searching MPPT control, which is popularly used in PV energy systems, is also studied in wind energy systems. P&O is based on a concept of perturbing the control variable in a small step-size and observing the results until the slope becomes zero. This method fails to follow the MPP trajectory under rapid wind variations because of the large moment of inertia in large WTs. A large step-size can be used to solve this issue but leads to more oscillations around the MPP [45].

A comprehensive comparison of various MPPT control techniques is summarized in Table 1.5 in terms of the input measurement variable(s) needed, prior knowledge of WT power characteristics needed, memory for storing the power curves, complexity of the overall control scheme, and performance of the algorithm with respect to varying wind-speed conditions. Overall, the OTSR and OT control techniques provide the best compromise between the complexity and performance.

Table 1.5 Summary of various MPPT control techniques [44, 45]

	Input Variable	Prior WT Knowledge	Memory Required	Complexity of Control	Control Performance
OTSR	v_w	Not Needed	No	Low	Very Good
WTPC	v_w	Needed	Yes	Medium	Very Good
OT	ω_m	Needed	No	Low	Good
PSF	ω_m	Needed	Yes	Medium	Good
GSF	$\mathbf{v_s}$, $\mathbf{i_s}$	Needed	Yes	Medium	Good
SSL	f_s	Needed	Yes	High	Good

1.7.5 Power Converter, Wind Generator, and Grid Control (Level I and II)

The block diagram of the overall control scheme depicted in Figure 1.22 indicates that the Level II control loop is related to the wind generator and grid control, and the Level I control loop corresponds to the power converter control. The Level I and II control loops are shown as two different blocks to clearly indicate the flow of the control variables. However, in reality, the Level I and II control loops are closely intertwined; thus, distinguishing them is difficult. To simplify the discussion, Level I is introduced first followed by Level II. To achieve high-energy conversion and feed the power to the grid, the following control objectives must be fulfilled in high-power WECS:

- MPPT under all wind-speed conditions.
- Net DC-bus voltage control to ensure proper operation for the GSC.
- RPG to meet the grid codes.

An accurate control of wind generators and power converters is necessary to fulfill the above control objectives. The first objective is achieved by the MSC/RSC, whereas the GSC handles last two objectives. Level II control produces the reference generator and grid currents ($\mathbf{i_s^*}$ and $\mathbf{i_g^*}$), and the Level I control produces switching signals ($\mathbf{s_r}$ and $\mathbf{s_i}$), such that the measured generator and grid currents ($\mathbf{i_s}$ and $\mathbf{i_g}$) follow their references ($\mathbf{i_s^*}$ and $\mathbf{i_g^*}$) closely.

The power flow between the wind generator and utility grid is also tightly regulated by the Level I control during both normal and grid fault conditions. In grid faults, the surplus energy between the generator and utility grid is dumped to the resistive load through a DC chopper, thus converting the kinetic energy of the turbine rotation into heat. The control system of the DC chopper dynamically adjusts the amount of energy to be dumped to the resistor. The DC chopper control subsystem reads the fault signal s_f value and generates the switching signal s_{ch} to the DC chopper such that the DC-link voltage v_{dc} never exceeds the upper threshold limit $v_{dc}^{\max}$.

(1) Power Converter Control (Level I): The development of digital control techniques for power converters is an ongoing research topic. A brief summary of classical and advanced control techniques for power converters is shown in Figure 1.27. Classical control techniques are well established in the literature and are widely employed to control converters, variable-speed drives, and energy conversion systems. The recent developments in digital control platforms such as μC, DSP, and FPGA enabled a designer/industry to develop more complex control algorithms to obtain optimal system performance. With the exponential increase in the computational capacity of digital control platforms, often expressed as million instructions per second (MIPS), the designer need not worry about the high number of calculations involved in the control algorithm. For example, the computational capacity offered by the TMS320C14 DSP in 1983 was limited to 10 MIPS, whereas the modern dSPACE DS1103 control platform can perform 2500 MIPS. The advanced control techniques improve the overall system performance by just software reconfiguration.

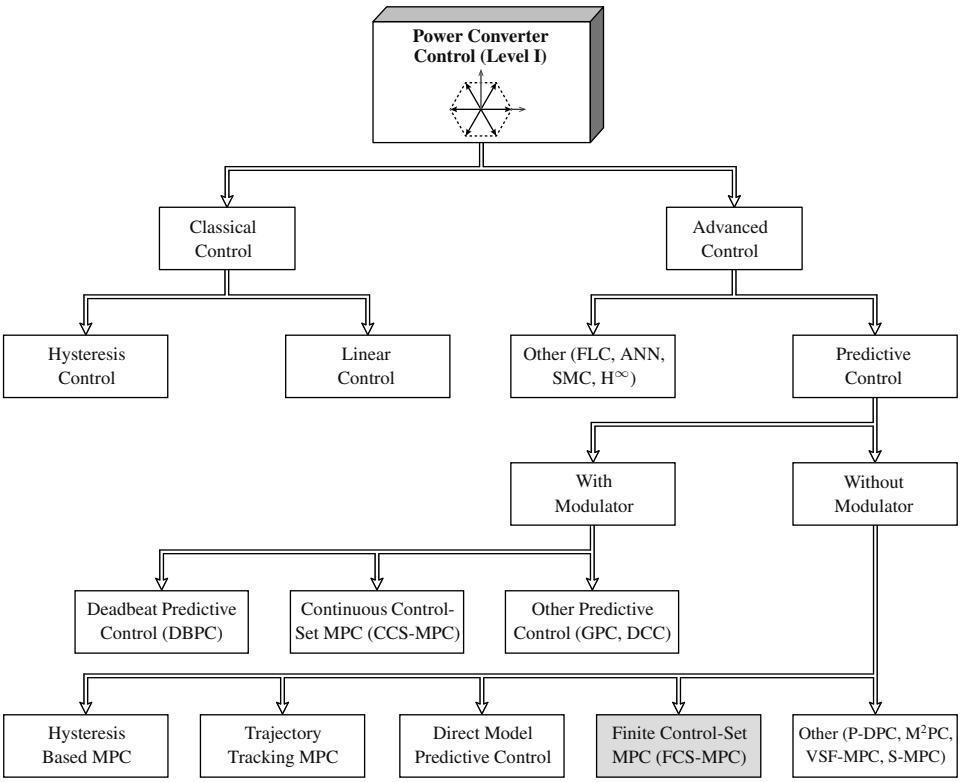

Figure 1.27 Taxonomy of power converter control techniques [48, 49]. (GPC, generalized predictive control; DCC, direct current control; P-DPC, predictive direct power control; M^2PC, modulated MPC; VSF-MPC, variable sampling frequency MPC; and S-MPC, switched MPC)

The classical control schemes include hysteresis (also known as bang–bang or on–off) control and linear control with modulation stage. The hysteresis control properly treats the nonlinear nature of the power converter. The bang–bang controller regulates the control variable x (current, torque, flux, active power, or reactive power) within the hysteresis band limits ($x^* \pm \delta/2$) and produces switching signals directly (or with the help of a lookup table in multivariable case) for the power converter with no intermediate modulation stage

[50]. On the basis of the variable to be controlled (x), the bang–bang control is used in different forms such as: (1) hysteresis current control to control the generator/grid currents, (2) direct torque control (DTC) to regulate the generator electromagnetic torque and stator flux , and (3) direct power control (DPC) to control the generator/grid active and reactive powers. These control strategies are simple to implement; however, the resultant switching frequency changes with respect to the operating conditions. The variable-switching frequency causes the harmonic spectrum to spread and might ignite resonance in some power converters. Over the years, several articles have been published to obtain constant switching frequency by combining hysteresis control with modulation stage. A very high sampling frequency is usually needed by the digital control platforms to implement hysteresis control.

The linear control with modulation stage treats the power converter as a linear model. In this approach, a PI controller (in most of the cases) regulates the control variable x (usually generator/grid current) at its reference value (x^*) by generating a reference voltage (modulation) signal v^* to the modulation stage. The modulation stage defines the switching actions for the power converter using the internal reference frame transformation and switching strategy. On the basis of the power converter topology, several modulation schemes are available: sinusoidal pulse-width modulation (SPWM), third harmonic injected PWM, space vector modulation (SVM), selective harmonic elimination, hybrid modulation, etc. [41]. SPWM and SVM are commonly used modulation schemes for power converters. SVM is preferred over SPWM because it offers better DC-bus utilization and produces a good load harmonic profile (power quality). However, SVM is complex compared with SPWM and involves a large number of calculations and reference frame transformations. A low switching frequency operation in power converters is an important requirement at a high-power level to minimize switching losses and allow proper heat dissipation. During such operations, a linear control with modulation imposes several technical and operational challenges. A few significant technical challenges are outlined below [51]:

- Unsymmetrical performance in different operating conditions as a linear controller is applied to the power converter that is nonlinear in nature.
- Significant lower-order harmonics are produced by the modulation stage that lead to poor power quality and conflict to the grid codes.
- Transient response becomes sluggish because of the low-bandwidth modulation stage.
- Control variables such as dq or $\alpha\beta$-axes generator/grid currents exhibit strong coupling. Thus, decoupling terms must be added with higher control complexity.
- Control performance degrades because of grid voltage harmonics and control delay.

Moreover, including system constraints such as THD, common-mode voltage minimization, and switching losses reduction is not straightforward in the design of a linear controller. For digital implementation, a designer needs to spend extra time to map the continuous-time (CT) linear controller to the discrete-time (DT) domain using sampled-data models. A favorable approach in using linear control with modulation is the fixed switching frequency (imposed by the carrier frequency in the modulation stage). The field-oriented control (FOC) for wind generators and voltage-oriented control (VOC) for grid-connected converters are high-end versions of the linear control.

Advanced and complex control schemes for power converters include fuzzy logic control, artificial neutral network-based control, neuro-fuzzy control, sliding-mode control, H^∞ control, and predictive control. The classical and advanced control schemes are reviewed further in Chapter 3. In the field of control engineering, predictive control has a

long history of development and applications since the 1950s. Initial applications include computer-based supervisory control projects by various oil and petrochemical industries [52]. In modern industrial controls, predictive control is a major success story, and this methodology has been used in hundreds of real-time applications. The predictive control concept for power converters was introduced during the 1980s; however, rigorous research has been conducted in recent years only because of the best responses (high computational capacity) provided by digital control platforms [53]. In the context of energy processing applications, predictive control offers a conceptually different and intuitive approach to control a power converter by treating it as a discontinuous and nonlinear actuator [6].

As outlined in Figure 1.27, predictive control covers a broad range of controllers with different control concepts. However, they all share a common philosophy: predict the future behavior of a control variable in each sampling instant by using the system model and select the optimal actuation based on the predefined optimization criteria [48]. Predictive control schemes can also be recognized as receding horizon controllers with one-sample-ahead prediction horizon. In power converters, predictive control is broadly classified into two categories based on whether a modulation stage is needed or not. DBPC, CCS-MPC, GPC, and DCC belong to the family of modulator-based predictive control schemes [49]. To reduce computational burden, optimizations are solved offline, producing a continuous control-set input variable (duty cycle or modulation index) to the modulation stage. The main advantages of modulator-based predictive control schemes are fast dynamic response and fixed switching frequency operation. However, these schemes are very sensitive to system parameter variations that could possibly lead to system instability.

The second category of predictive control techniques, including hysteresis-based MPC, trajectory-tracking MPC, direct MPC, and finite control-set MPC operate without any modulator; therefore, the switching frequency is not constant. The actuation from these control schemes is optimal switching signals which have a finite (discrete) control-set nature. Hysteresis-based MPC forces the control variable to remain in the hysteresis boundaries (similar to the hysteresis current control), whereas in trajectory-tracking MPC, the control variable follows the predefined control trajectory (similar to the sliding-mode current control). Direct MPC allows long prediction horizons to improve overall control performance. In recent years, FCS-MPC has emerged as a simple, intuitive, powerful, and promising alternative to control power converters that have a finite number of switching states [54]. FCS-MPC replaces the cascaded control structure and modulation stage and provides a fast and dynamic response in addition to good steady-state reference tracking. This technique offers simplicity and great flexibility for a designer to incorporate several control objectives by simply changing the optimization criteria (cost function). One of the best features of the FCS-MPC strategy is that system nonlinearities and limitations can be incorporated directly into the system model. FCS-MPC operates with variable-switching frequency similar to hysteresis control; however, a designer can control the number of switch changes (switching frequency) by imposing a restriction in the cost function. The finite control-set model predictive control is the subject of this book.

Some research has combined the operating principles of MPC and SVM to obtain the best qualities of each class: fast dynamic response as in MPC and constant switching frequency as in SVM. A few of these novel control strategies were introduced very recently in 2015: P-DPC [55], M^2PC [56, 57], VSF-MPC [58], and S-MPC [59]. These strategies employ predefined power converter voltage space vector sequences in the modeling of the system. These control schemes are relatively new and premature, hence they are not discussed in the reminder of this book.

(2) Wind Generator and Grid Control (Level II): The design, construction, operation, and control of a wind generator and electric motor are similar. Based on the sign of mechanical input torque T_m, an electric machine can be used as a generator or motor (negative T_m for generator and positive T_m for motor). All theories and practical developments in electric motor control can therefore be attributed to wind generator control. In comparison to electric motors control, the wind generators employ additional MPPT control loop to generate reference speed ω_m^*, reference torque T_e^*, or reference power P_s^*. The wind generator control schemes mentioned in this book are derived from the electric motor control theory that is well documented in literature. Wind generator control schemes are broadly classified into two classes: classical control and predictive control. The taxonomy of wind generator control schemes is presented in Figure 1.28 considering both IGs and SGs.

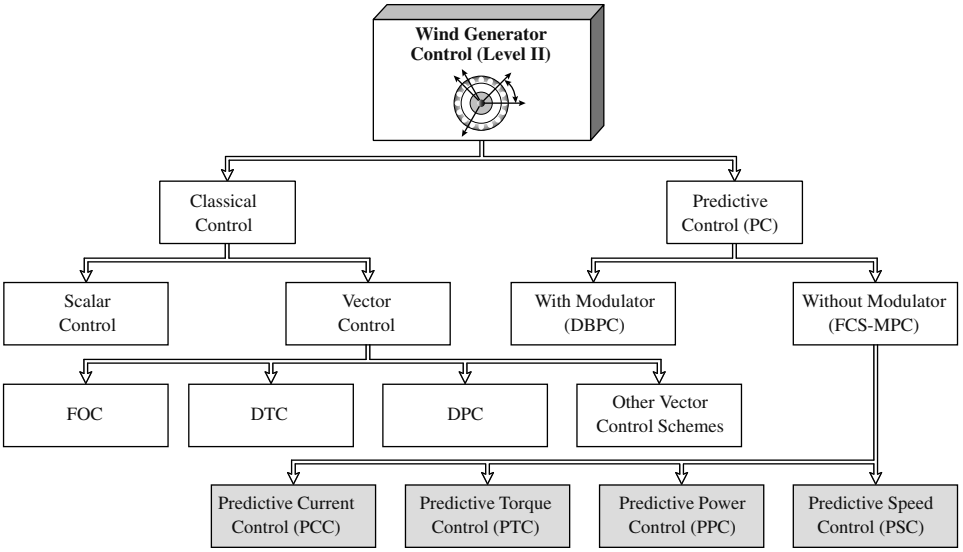

Figure 1.28 Taxonomy of wind generator control techniques [60].

Scalar and vector control techniques form classical control schemes, and the latter is extensively used in electric drives and the wind energy industry. In scalar control, only the magnitude and frequency of space vector (voltage, current, or flux linkage) is adjustable; therefore, an acceptable performance is guaranteed during steady-state operation. In vector control, in addition to magnitude and frequency, the instantaneous position (phase angle) of the space vector is controlled; as a result, a high-performance operation is obtained in both steady-state and transient conditions. Vector control of a wind generator is a general and decoupled control philosophy that can be further classified as FOC, DTC, DPC, and other forms, such as feedback linearization control and passivity-based control [60]. Vector control schemes are implemented by transforming the generator dynamic equations into field coordinates that rotate in synchronism with the rotor or stator flux or voltage vector. The FOC for SCIG and SG uses rotor flux orientation; FOC for DFIG uses stator flux or voltage orientation; and DTC uses stator flux orientation. It has been well established in the literature that field coordinates provide decoupled control in AC machines similar to the separately excited DC machine. As mentioned earlier, FOC of wind generator and VOC of GSC belong to the class of linear control schemes, and the DTC and DPC belong to the nonlinear hysteresis control.

FOC and DTC are two frequently-used methods in the present industry to obtain high control performance [61]. In the FOC scheme, wind generator three-phase currents are transformed into two orthogonal components that define the magnetic flux and electromagnetic torque. To force the measured currents to follow their reference currents, two PI controllers are used to generate a reference voltage vector for the modulation stage. The modulation stage compares the reference voltages with the carrier waveform and generates switching signals for the power converter. FOC is a linear control method, and its switching frequency is constant (set by modulator). FOC schemes are available in two forms: direct or feedback FOC (DFOC or *Blaschke* control) and indirect or feed-forward FOC (IFOC or *Hasse* control). The latter is widely used because of its simplicity throughout the speed range. The rotor field-oriented FOC is used to control SCIG, stator field-oriented FOC is employed in DFIG, and rotor flux-oriented maximum torque per ampere control (essentially FOC scheme) is used in PMSG [13].

DTC represents a viable alternative to the FOC scheme. Instead of a decoupled generator current control, the DTC scheme directly controls the generator stator flux and electromagnetic torque by employing hysteresis comparators and a lookup table. The required flux and torque are computed on the basis of measured generator voltages and currents. In comparison with FOC, the DTC scheme is relatively simple and eliminates the need for coordinate transformation, PI controllers, and pulse-width modulation. However, the number of online calculations with DTC is higher than FOC, thus making DTC a highly computational intensive control. Classical DTC is a nonlinear control and operates with variable-switching frequency. DTC control is available in two forms based on the selection of switching sectors: circular stator flux DTC (*Takahashi* and *Noguchi* control) and hexagonal stator flux (*Depenbrock* control). The DTC technique has been applied to SCIG, DFIG, and interior PMSG (IPMSG). In the DPC method, the generator active and reactive powers are controlled by hysteresis comparators and a lookup table, similar to DTC.

The operating principles of FOC, DTC, and DPC vector control schemes are used by FCS-MPC to design predictive current control (PCC), predictive torque control (PTC), and predictive power control (PPC), respectively. All control variables of FOC, DTC, and DPC are regulated by PCC, PTC, and PPC without employing any internal PI or hysteresis controllers. All model predictive control schemes are modulation-stage free; thus switching frequency is variable. In both classical and predictive control schemes, the outer speed control loop employs a PI controller to regulate the generator speed at its reference value. The PCC, PTC, and PPC schemes only replace the internal control loops of FOC, DTC, and DPC schemes respectively that need faster control actions than the sluggish outer speed control loop. The predictive speed control (PSC) scheme represents a recent development in this area. This scheme eliminates the speed PI controller and internal PI controllers, thus making it a completely cascade-free control structure [62]. This approach uses PCC, PTC, or PPC internally to simultaneously control the generator speed and control variables. Compared with PCC, PTC, and PPC, the control complexity of PSC increases slightly because of higher-order modeling and *ad hoc* cost function definition.

GSCs in variable-speed WECS are controlled by decoupled VOC or DPC [50]. In VOC, through the regulation of orthogonal-axis grid currents, the net DC-bus voltage (active power) and reactive power are controlled, respectively. In the DPC scheme, similar to the generator-side control scheme, the grid active and reactive powers are controlled independently. In summary, the main objectives for both classical vector control and predictive control schemes is to regulate independently: (1) the orthogonal-axis currents in FOC/VOC/PCC schemes, (2) generator torque and flux in DTC/PTC schemes, and (3) active and reactive powers in DPC/PPC of wind generator or GSC.

1.8 FINITE CONTROL-SET MODEL PREDICTIVE CONTROL

FCS-MPC offers several advantages that make it suitable for the optimal control of power converter-based energy processing applications [6]. FCS-MPC is an attractive solution for researchers in the industry and academe. Recent scholarly works demonstrated that FCS-MPC can easily be applied to a wide range of power converters with different output harmonic filter configurations, adjustable-speed motor drives, power quality, HVDC, and wind and PV energy conversion applications [63]. These features come with few technical challenges (research opportunities) that need to be addressed. In this section, the main features and challenges of FCS-MPC are analyzed in detail.

1.8.1 Main Features of FCS-MPC

As illustrated in Figure 1.29, the main features of the FCS-MPC are classified into eight categories. A brief description of these main features is presented below.

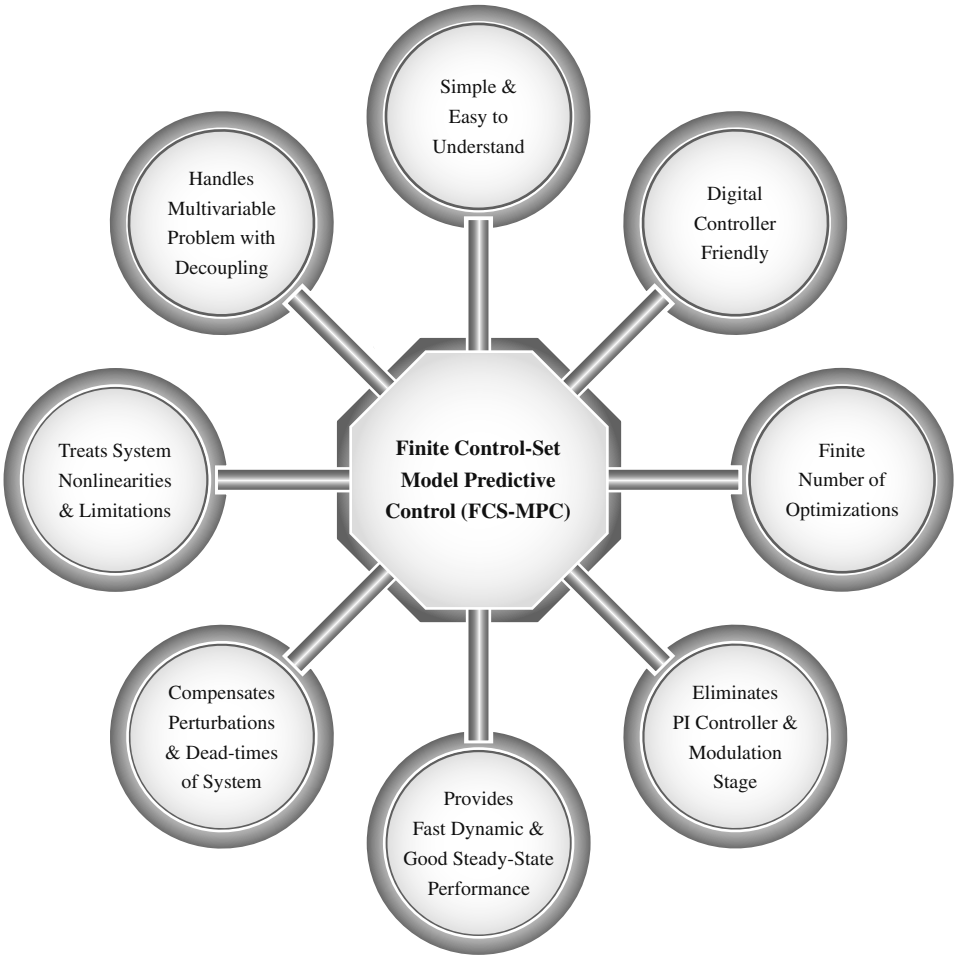

Figure 1.29 Main features of finite control-set model predictive control.

(1) Simple and Easy to Understand: FCS-MPC uses a simple concept, and it is easy to understand. Regardless of control application, FCS-MPC always uses four main subsystems, as presented below:

- **References Calculation:** This subsystem calculates the reference control variable $\mathbf{x}^*(k)$ ($\mathbf{x} \in$ voltage, current, power, torque, flux, etc.) according to the type of application. The references calculation is a common design step for classical and MPC schemes.
- **Extrapolation:** In this subsystem, the future value of the reference control variable $\widehat{\mathbf{x}}^*(k+1)$ is estimated based on the present and past sample values ($\mathbf{x}^*(k)$, $\mathbf{x}^*(k-1)$, etc.), or based on present sample value and angle of reference frame ($\mathbf{x}^*(k)$ and $\theta^*(k)$).
- **Predictive Model:** Possible future values of control variables $\mathbf{x}^{\mathbf{P}}(k+1)$ are predicted by this subsystem based on DT model and parameters of system, feedback signal values, and converter switching state combinations, $\mathbf{s}(k)$.
- **Cost Function Minimization:** The error between the predicted and extrapolated control variable $g = \widehat{\mathbf{x}}^*(k+1) - \mathbf{x}^{\mathbf{P}}(k+1)$ is calculated by this subsystem. The switching state $\mathbf{s}(k)$ that produces the "minimum" cost function error is selected as an optimal actuation (output) of FCS-MPC, and the output is applied to the power converter directly.

According to the application, additional blocks in FCS-MPC can appear; however, these blocks assist main subsystems. For example, a reference frame transformation block converts three-phase generator/grid currents into orthogonal components.

(2) Digital Controller Friendly: The inherent and discrete nature of power converters is considered in the design of a "predictive model" subsystem of FCS-MPC. Simulation models of FCS-MPC execute the algorithm with a discrete step size; consequent analysis of the control scheme is conducted in a DT domain. Real-time implementation of FCS-MPC by digital control platforms is, therefore, intuitive and natural. Hence, the time required for a designer to switch from a simulation stage to a real-time implementation stage is negligible; thus the overall FCS-MPC design framework is simple.

(3) Finite Number of Optimizations: FCS-MPC is a model-based optimization algorithm that performs a set of calculations during each sampling period. The number of iterations in the optimization algorithm are determined according to the possible number of converter switching states $\mathbf{s}(k)$. The power semiconductor switch in any converter possesses two discrete states: *turn-on* ('1') or *turn-off* ('0'). Thus the number of switching combinations (switching states) in any converter are limited to a finite set. For example, 8 and 27 switching states are available for 2L-VSC and NPC converter, respectively. Optimizations are greatly simplified because of the finite number of switching states, making it possible to implement FCS-MPC by digital control platforms available in the market.

(4) Eliminates PI Controller and Modulation Stage: FCS-MPC uses the DT model of system to predict the future behavior of control variables for every possible actuation sequence. Cost function minimization is used as an optimization criteria to evaluate system performance for all possible switching states. An optimal switching state that minimizes the cost function is directly applied to the converter. This approach eliminates the need for linear PI controllers, hysteresis regulators, intermediate modulation stage, and the lookup table in the control loop. FCS-MPC is a nonlinear control method, and it provides a better approach to control the power converters that are also nonlinear in nature.

(5) Provides Fast Dynamic and Good Steady-State Performance: Linear control techniques, such as FOC and VOC, treat the power converter as a linear actuator. The nonlinear nature of the power converter becomes more predominant at a lower switching frequency operation. Under such conditions, FCS-MPC provides better control in dynamic response and steady-state reference tracking. The resultant dynamic performance of FCS-MPC is superior to linear control because of the elimination of the low-bandwidth modulation stage.

(6) Compensates Perturbations and Dead-Times of System: Power conversion system perturbations, power converter dead-times, and on-state voltage drop of semiconductor switches are easily compensated by FCS-MPC. Although the output harmonic filter and internal DC-link filter parameters change, the controller can mitigate the perturbations by choosing a switching state that produces the minimal cost function error. Reference tracking is slightly affected by system perturbations; however, the transient response remains fast compared with linear control.

(7) Treats System Nonlinearities and Limitations: FCS-MPC treats various power converter topologies as discontinuous and nonlinear actuators that are the closest approximations to a real-time scenario. One of the best features of FCS-MPC is that the nonlinearities and limitations of the power converter can be incorporated directly into the system model. The cost function definition is flexible; several constraints and technical requirements such as maximum current limitation, switching frequency reduction, spectrum shaping, common-mode voltage minimization, power losses reduction, THD, boundary limits for electrical and mechanical variables, etc., can be incorporated in the design and operation of the controller to achieve a safe and reliable operation.

(8) Handles Multivariable Problem with Decoupling: For a wide variety of systems, FCS-MPC handles multivariable control problems in a decoupled manner without employing compensation terms outside the control loop. The "soft constraint" and "hard constraint" handled in a multivariable control framework is naturally accommodated by FCS-MPC through proper selection of weighting factors. This feature is particularly preferred in electromechanical energy conversion applications where both electrical and mechanical control variables need to be handled by FCS-MPC.

1.8.2 Challenges of FCS-MPC

Despite the simplicity and benefits of FCS-MPC, several challenges exist in state-of-the-art research that include, but not limited to:

(1) Large Number of Calculations: FCS-MPC performs a large number of online calculations during each sampling interval, thus leading to higher computational burden than the linear control scheme. This finding was a major obstacle for digital control designers until the last decade. However, modern DSPs can perform extensive calculations at a reduced cost. For example, the FCS-MPC for 2L-VSC (8 switching states), 3L-DCC (27 states), 4L-DCC (64 states), and 5L-DCC (125 states) can be realized with a minimum execution time (T_s) of 7, 18, 44, and 93 μs, respectively [8]. With the industry standard microprocessors, more freedom is obtained in the simultaneous control of BTB connected power converters. For some power converter topologies such as CHB and MMC, the number of switching states increases exponentially with the number of modules in each phase. To develop FCS-MPC with less computational burden, the closest vectors to the reference voltage vector should be selected, which is similar to the methodology employed in SVM.

(2) Variable-Switching Frequency: The main drawback of FCS-MPC compared with the linear control is that the converter switching frequency varies with respect to the operating conditions. This finding leads to spread spectrum in the control variable harmonic profile. The cost function can be penalized to control the switching frequency to some extent. For example, the average switching frequency of the converter can be regulated between two close boundary limits by the online adjustment of weighting factors [64].

(3) Heuristic Selection of Weighting Factors: The cost function in FCS-MPC includes several control objectives (variables) simultaneously. The relative importance of one objective over the other can be set through the weighting factors. Control variables possess different physical natures (current, voltage, power, etc.), and these variances lead to coupling effects; thus the selection of suitable weighting factors becomes tedious. The numerical procedure for the weighting factor selection is still an open research topic; however, some guidelines can be found in the literature [65]. In this book, a few case studies are designed to establish the theoretical framework for the calculation of weighting factors.

(4) Need for Accurate Model of System: The control performance obtained by the FCS-MPC depends greatly on the DT system model and prediction horizon. In the field of power electronics, CT mathematical models of various power converters and wind generators that are highly accurate and precise are readily available. Mapping CT models to the DT models is a mature subject matter in the field of control theory. In the current literature, DT models for various power conversion-related applications are well documented. For linear time-varying CT (for example, induction, and synchronous machine) models, calculation of corresponding exact DT models is impossible. In such cases, approximate models with high precision improve the system performance [66].

The challenges of using FCS-MPC that are related to the nature of the control of variable-switching frequency, weighting factors selection, control delay compensation, and robustness analysis are properly addressed in this book.

1.9 CLASSICAL AND MODEL PREDICTIVE CONTROL OF WECS

This section demonstrates the conceptual difference between classical FOC and PCC of variable-speed WECS. A Type 4 WECS with PMSG and BTB 2L-VSC is considered. To simplify the analysis, only the generator-side control scheme is presented considering Levels I to III control loops.

Stator voltage and electromagnetic torque dynamics of a permanent magnet synchronous machine (motor case) are described in the synchronous (dq) reference frame as

$$v_{ds} = R_s\, i_{ds} - \omega_r\, L_{qs}\, i_{qs} + L_{ds}\frac{d\, i_{ds}}{dt} \tag{1.10}$$

$$v_{qs} = R_s\, i_{qs} + \omega_r\, L_{ds}\, i_{ds} + L_{qs}\frac{d\, i_{qs}}{dt} + \omega_r\, \psi_r \tag{1.11}$$

$$T_e = 1.5\, P_p\, [\psi_r\, i_{qs} + (L_{ds} - L_{qs})\, i_{ds}\, i_{qs}] \tag{1.12}$$

where v_{ds} and v_{qs} are machine stator voltages in dq frame, i_{ds} and i_{qs} are machine dq frame stator currents, ψ_r is the peak value of rotor flux linkage produced by permanent magnets, R_s is the machine stator resistance, L_{ds} and L_{qs} are machine dq-axes inductances, ω_r is the rotor electrical speed, and P_p is the machine number of pole pairs.

As mentioned earlier, a motor model can be used for generator control by simply measuring the currents in opposite direction. To simplify the analysis, PMSG is assumed to have surface permanent magnet (non-salient-pole) configuration with $L_{ds} = L_{qs} = L_s$. FOC and PCC of PMSG WECS with a generator-side two-level voltage source rectifier (2L-VSR) is presented below, assuming that the GSC regulates the net DC-bus voltage and grid reactive power. Grid-side control scheme has an identical concept for both the classical and predictive control.

1.9.1 Classical Control of WECS

The block diagram of the classical FOC scheme is shown in Figure 1.30. The CT feedback measurements, such as three-phase generator currents $\mathbf{i_s}$, DC-link voltage v_{dc}, generator speed and position (ω_m and θ_m), and wind speed v_w are interfaced to the digital control through analog-to-digital converter (ADC) channels. Switching signals $\mathbf{s_r}$ produced by the digital control are sent to the 2L-VSR through the digital input/output channel and interface board containing a signal conditioner and gate drivers.

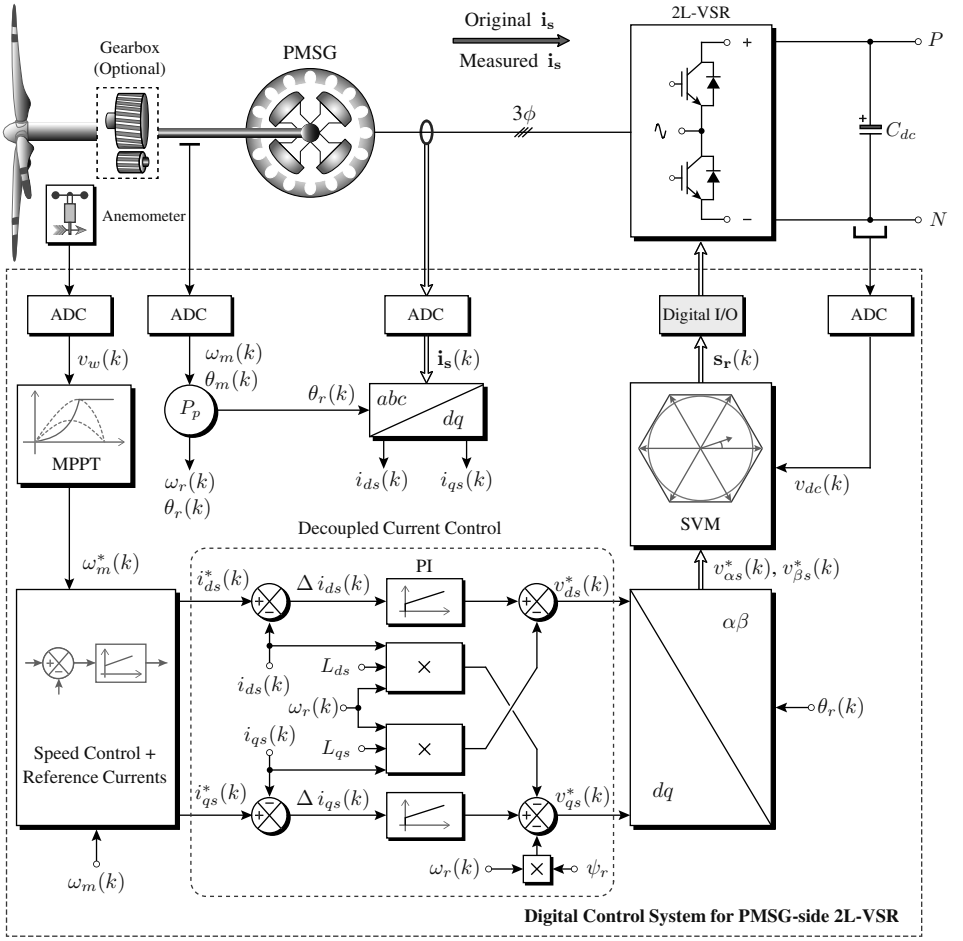

Figure 1.30 Classical zero d-axis current control of 2L-VSR-based PMSG WECS.

OTSR MPPT control produces reference speed ω_m^* based on varying v_w input values, such that the turbine operates at the optimal tip speed ratio λ_T^{op}. Mechanical speed and position values (ω_m and θ_m) are converted to corresponding electrical values (ω_r and θ_r) by multiplying these with the generator number of pole pairs. The three-phase currents are converted to dq-axes to facilitate control algorithm implementation in synchronous frame. The digital control uses cascaded control structure with an outer speed control loop and inner current control loop. The PI controller in the speed control loop regulates ω_m at its reference value ω_m^*, and the output of this loop is reference electromagnetic torque, T_e^*. Based on (1.12), electromagnetic torque production in PMSG is proportional to i_{qs} when $L_{ds} = L_{qs}$. With this criteria, d-axis reference current i_{ds}^* is set to zero, and the q-axis reference current i_{qs}^* is calculated from T_e^*, that is,

$$i_{ds}^* = 0, \qquad i_{qs}^* = \frac{T_e^*}{1.5\, P_p\, \psi_r}. \tag{1.13}$$

For this reason, the rotor flux-oriented FOC of PMSG is called zero d-axis current (ZDC) control. In this control, a linear relationship between torque and stator current is obtained when rotor flux linkage ψ_r is kept constant. This operation is identical to the separately excited DC machine, where field flux is maintained constant and torque is controlled by varying armature current [13].

The feedback dq-axis currents i_{ds} and i_{qs} are compared with their reference currents i_{ds}^* and i_{qs}^*, respectively. Error currents Δi_{ds} and Δi_{qs} are sent to two PI controllers. The output of the PI controller in the d-axis loop along with compensation term $\omega_r L_{qs} i_{qs}$ is used to calculate d-axis reference voltage v_{ds}^*. Similarly, q-axis reference voltage v_{qs}^* is calculated as a summation of the q-axis loop PI controller output and compensation terms $\omega_r L_{ds} i_{ds}$ and $\omega_r \psi_r$. Stator winding resistance R_s is negligible in high-power generators; hence the terms $R_s i_{ds}$ and $R_s i_{qs}$ are not included in the compensation terms. The compensation terms in dq-axes loops provide decoupled control for i_{ds} and i_{qs} while improving the performance during transient conditions [67]. The 2L-VSR synchronous frame reference voltages v_{ds}^* and v_{qs}^* are transformed into stationary frame reference voltages via $dq/\alpha\beta$ transformation using electrical position angle θ_r. More details about the reference frame transformation are presented in Chapter 3.

The two-phase sinusoidal reference voltages $v_{\alpha s}^*$ and $v_{\beta s}^*$ are used by the SVM stage. The SVM stage involves a large number of internal calculations to produce three-phase gating signals $\mathbf{s_r}$, such that the MPPT is achieved during each sampling interval. With the successful MPPT, the generator current, electromagnetic torque, and rotational speed are strictly regulated.

1.9.2 Model Predictive Control of WECS

The block diagram of the predictive current control scheme for a 2L-VSR-based PMSG WECS is shown in Figure 1.31. The control scheme is very easy to understand. It consists of four main subsystems: reference currents calculation, extrapolation, predictive model, and cost function minimization. Notation of variables, calculation of reference speed ω_m^*, and reference currents i_{ds}^* and i_{qs}^* is similar to the ZDC control discussed earlier. Once the reference currents are obtained in $(k)^{\text{th}}$ instant, these are extrapolated to $(k+1)$ sampling instant for use with the cost function. The PCC scheme replaces the decoupled PI controller, $dq/\alpha\beta$ transformation, and SVM stage. PCC considers one-sample-ahead prediction horizon to simplify the analysis.

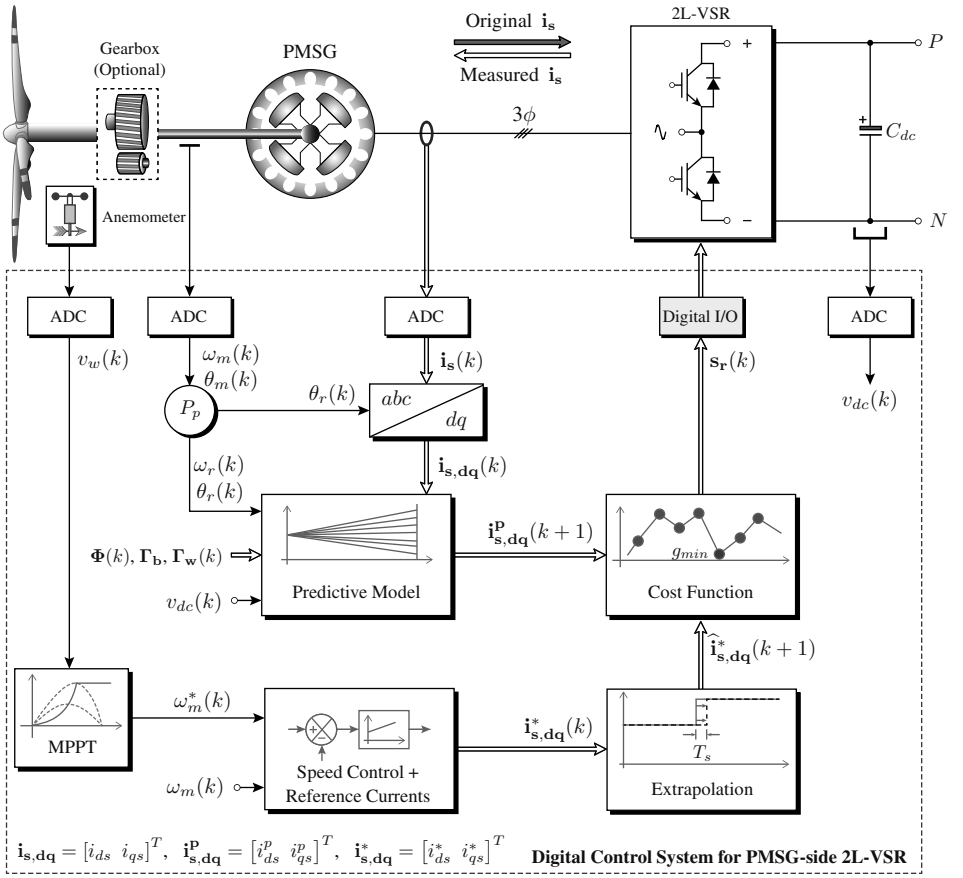

Figure 1.31 Predictive current control of 2L-VSR-based PMSG WECS.

PCC uses the DT model of PMSG and 2L-VSR to predict the future behavior of generator currents. Using the PMSG stator voltage models given in (1.10) and (1.11), the DT model of generator dq-axes currents is obtained by forward Euler approximation as follows:

$$\begin{bmatrix} i^p_{ds}(k+1) \\ i^p_{qs}(k+1) \end{bmatrix} = \underbrace{\begin{bmatrix} 1-\frac{R_s\,T_s}{L_s} & \omega_r(k)\,T_s \\ -\omega_r(k)\,T_s & 1-\frac{R_s\,T_s}{L_s} \end{bmatrix}}_{\mathbf{\Phi}(k)} \begin{bmatrix} i_{ds}(k) \\ i_{qs}(k) \end{bmatrix} + \underbrace{\begin{bmatrix} \frac{T_s}{L_s} & 0 \\ 0 & \frac{T_s}{L_s} \end{bmatrix}}_{\mathbf{\Gamma_b}} \underbrace{\begin{bmatrix} v^p_{ds}(k) \\ v^p_{qs}(k) \end{bmatrix}}_{\text{2L-VSR Model}}$$
$$+ \underbrace{\begin{bmatrix} 0 \\ -\frac{\omega_r(k)\,\psi_r\,T_s}{L_s} \end{bmatrix}}_{\mathbf{\Gamma_w}(k)}, \qquad \underbrace{\begin{bmatrix} v^p_{ds}(k) \\ v^p_{qs}(k) \end{bmatrix}}_{\text{2L-VSR Model}} = v_{dc}(k) \begin{bmatrix} s^p_{dr}(k) \\ s^p_{qr}(k) \end{bmatrix} \tag{1.14}$$

where T_s is sampling time. The subscript p denotes the predicted variable. As shown in the expression above, future generator currents are predicted based on the measured i_{ds}, i_{qs}, and v_{dc}, generator parameters R_s and L_s, and predicted 2L-VSR voltages v^p_{ds} and v^p_{qs}. The DT parameter matrix $\mathbf{\Gamma_b}$ can be calculated offline; however, $\mathbf{\Phi}(k)$ and $\mathbf{\Gamma_w}(k)$ must be computed online based on $\omega_r(k)$ measurement. The prediction of 2L-VSR voltages

uses eight possible switching states (represented in a synchronous reference frame) and the measured DC-link voltage, v_{dc}. Based on this state-space model, the future behavior of the generator currents is controlled by properly choosing an optimal one among the eight possible switching states.

The control objective is to regulate i_{ds} and i_{qs} at their reference values i^*_{ds} and i^*_{qs}, respectively. As the final stage, a cost function is defined to fulfill the control objective:

$$g(k) = \left[\widehat{i}^*_{ds}(k+1) - i^p_{ds}(k+1)\right]^2 + \left[\widehat{i}^*_{qs}(k+1) - i^p_{qs}(k+1)\right]^2. \tag{1.15}$$

The ideal minimum of the cost function is zero that represents the perfect regulation of the generator currents. During each sampling instant, switching signals that minimize the cost function in (1.15) are chosen and applied to the 2L-VSR directly. Additional constraints such as generator current limitation during transient condition, switching frequency minimization, common-mode voltage mitigation, etc., can also be included in the cost function with suitable weighting factors. A fast dynamic response is guaranteed by PCC because it eliminates the linear PI controllers and SVM stage.

1.9.3 Comparison of Classical and Model Predictive Control

Classical and model predictive control schemes are compared based on abstract details given in the previous two sections and summarized, as shown in Table 1.6 [68]. The classical DTC and PTC are also included for the sake of comparison although these have not been analyzed in detail in this chapter. The digital control schemes are compared based on the nature of controller, critical design stage, requirement for modulation stage, control complexity, computational burden (number of online calculations), nature of converter switching frequency, and performance during transient conditions.

Switching frequency is constant with classical FOC, and all other control schemes operate with variable-switching frequency. The steady-state response obtained in all the methods is more or less same. The dynamic response obtained by predictive control schemes is better compared to classical FOC and DTC. In general, the model predictive control provides opportunities for a designer or industry to control wind generators and power converters in a simple manner.

Table 1.6 Summary of comparison between classical and predictive control schemes [68]

	Classical FOC	**Classical DTC**	**Predictive FOC (PCC)**	**Predictive DTC (PTC)**
Control Scheme	Figure 1.30	–	Figure 1.31	–
Nature of Controller	Linear	Nonlinear	Nonlinear	Nonlinear
Critical Design Stage	PI + Modulation	Lookup Table	Cost Function	Cost Function
Modulation Stage	PWM/SVM	Not Required	Not Required	Not Required
Control Complexity	Very High	High	Low	Low
Computational Burden	Moderate	Very High	High	High
Switching Frequency	Fixed	Variable	Variable	Variable
Transient Response	Moderate	Good	Excellent	Excellent

1.10 CONCLUDING REMARKS

In this chapter, a comprehensive review of high-power wind energy systems is presented with respect to cumulative and annual installed capacity, wind energy popularity around the globe, principle of wind kinetic energy to electric energy conversion, various classes of WT technologies, major mechanical and electrical components of MW-WECS, fixed- and variable-speed operation of WECS, overall control of WECS, main features and challenges of FCS-MPC, and classical and model predictive control of WECS. A detailed technical background on WT power curves, aerodynamic power regulation including pitch control, TSR concept, grid code requirements such as FRT and RPG, MPPT control schemes, grid integration, wind generator and power converter control is also presented.

Link to Next Chapters:

The material in this chapter will complement the in-depth technical analysis to be conducted in other chapters of this book. The generator–converter configurations presented in Section 1.5 are discussed further in Chapter 2 with respect to power converter topologies for Types 3 and 4 variable-speed WECS. The WECS control discussed in Section 1.7 is studied again in Chapters 3 and 4 with more focus on electrical control systems and the fundamentals of model predictive control. The IGs and SGs presented in Section 1.3.2 are further studied in Chapter 6 for modeling and model predictive control.

REFERENCES

1. V. Yaramasu, B. Wu, P. C. Sen, S. Kouro, and M. Narimani, "High-power wind energy conversion systems: State-of-the-art and emerging technologies," *Proceedings of the IEEE*, vol. 103, no. 5, pp. 740–788, May 2015.
2. Global Wind Energy Council (GWEC), "Global wind report: Annual market update," 2014, available at: http://www.gwec.net, accessed on April 2015.
3. Renewable Energy Policy Network for the 21st Centuray (REN21), "Renewables 2014: Global status report," 2014, available at: http://www.ren21.net, accessed on April 2015.
4. Navigant Research, "A BTM wind report: World wind energy market update," 2015, available at: http://www.navigantresearch.com, accessed on April 2015.
5. F. Blaabjerg and K. Ma, "Future on power electronics for wind turbine systems," *IEEE Journal of Emerging and Selected Topics in Power Electronics*, vol. 1, no. 3, pp. 139–152, September 2013.
6. J. Rodriguez and P. Coftes, *Predictive Control of Power Converters and Electrical Drives*, 1st ed. Chichester, UK: IEEE Wiley Press, March 2012.
7. L. Wang, S. Chai, D. Yoo, L. Gan, and K. Ng, *PID and Predictive Control of Electrical Drives and Power Converters using MATLAB/Simulink*. Singapore: Wiley-IEEE Press, March 2015.
8. V. Yaramasu, "Predictive control of multilevel converters for megawatt wind energy conversion systems," Ph.D. Dissertation, Ryerson University, Toronto, ON, Canada, 2014, available at: http://digital.library.ryerson.ca/islandora/object/RULA%3A3459.
9. C. Carrillo, A. Obando Montaño, J. Cidrás, and E. Díaz-Dorado, "Review of power curve modelling for wind turbines," *Renewable and Sustainable Energy Reviews*, vol. 21, pp. 572–581, 2013.
10. J. Earnest and T. Wizelius, *Wind Power Plants and Project Development*. New Delhi, India: PHI Learning, May 2011.
11. Z. Chen, J. Guerrero, and F. Blaabjerg, "A review of the state of the art of power electronics for wind turbines," *IEEE Transactions on Power Electronics*, vol. 24, no. 8, pp. 1859–1875, August 2009.
12. E. Muljadi and C. Butterfield, "Pitch-controlled variable-speed wind turbine generation," *IEEE Transactions on Industry Applications*, vol. 37, no. 1, pp. 240–246, January 2001.
13. B. Wu, Y. Lang, N. Zargari, and S. Kouro, *Power Conversion and Control of Wind Energy Systems*, 1st ed., ser. IEEE Press Series on Power Engineering. Hoboken, NJ: Wiley-IEEE Press, July 2011.
14. J. Guerrero, F. Blaabjerg, T. Zhelev, K. Hemmes, E. Monmasson, S. Jemei, M. Comech, R. Granadino, and J. Frau, "Distributed generation: Toward a new energy paradigm," *IEEE Industrial Electronics Magazine*, vol. 4, no. 1, pp. 52–64, March 2010.

15. P. Bresesti, W. Kling, R. Hendriks, and R. Vailati, "HVDC connection of offshore wind farms to the transmission system," *IEEE Transactions on Energy Conversion*, vol. 22, no. 1, pp. 37–43, March 2007.

16. The European Wind Energy Association (EWEA), "Offshore wind," 2014, available at: http://www.ewea.org, accessed on April 2015.

17. H. Li and Z. Chen, "Overview of different wind generator systems and their comparisons," *IET Renewable Power Generation*, vol. 2, no. 2, pp. 123–138, June 2008.

18. M. Liserre, R. Cardenas, M. Molinas, and J. Rodríguez, "Overview of multi-MW wind turbines and wind parks," *IEEE Transactions on Industrial Electronics*, vol. 58, no. 4, pp. 1081–1095, April 2011.

19. International Renewable Energy Agency (IRENA), "Renewable energy technologies: Cost analysis series – wind power," vol. 1: Power Sector, no. 5/5, June 2012, available at: http://www.irena.org/, accessed on April 2015.

20. European Commision, "2013 JRC wind status report: Technology, market and economic aspects of wind energy in Europe," available at: http://setis.ec.europa.eu/, accessed on April 2015.

21. H. Polinder, J. Ferreira, B. Jensen, A. Abrahamsen, K. Atallah, and R. McMahon, "Trends in wind turbine generator systems," *IEEE Journal of Emerging and Selected Topics in Power Electronics*, vol. 1, no. 3, pp. 174–185, September 2013.

22. J. A. Baroudi, V. Dinavahi, and A. M. Knight, "A review of power converter topologies for wind generators," *International Journal of Renewable Energy*, vol. 32, no. 14, pp. 2369–2385, 2007.

23. Z. Zhu and J. Hu, "Electrical machines and power-electronic systems for high-power wind energy generation applications: Part I – market penetration, current technology and advanced machine systems," *COMPEL: The International Journal for Computation and Mathematics in Electrical and Electronic Engineering*, vol. 32, no. 1, pp. 7–33, 2013.

24. F. Blaabjerg, M. Liserre, and K. Ma, "Power electronics converters for wind turbine systems," *IEEE Transactions on Industry Applications*, vol. 48, no. 2, pp. 708–719, March 2012.

25. F. Blaabjerg, R. Teodorescu, M. Liserre, and A. Timbus, "Overview of control and grid synchronization for distributed power generation systems," *IEEE Transactions on Industrial Electronics*, vol. 53, no. 5, pp. 1398–1409, October 2006.

26. W. Erdman and M. Behnke, *Low Wind Speed Turbine Project Phase II: The Application of Medium-Voltage Electrical Apparatus to the Class of Variable Speed Multi-Megawatt Low Wind Speed Turbines*. National Renewable Energy Laboratory (N.R.E.L.), Golden, CO, USA, 2012.

27. M. Tsili and S. Papathanassiou, "A review of grid code technical requirements for wind farms," *IET Renewable Power Generation*, vol. 3, no. 3, pp. 308–332, September 2009.

28. E.ON Netz Gmbh, "Grid code – high and extra high voltage," April 2006.

29. F. Iov, A. D. Hansen, P. Sorensen, and N. A. Cutululis, "Mapping of grid faults and grid codes," Riso National Laboratory, Technical University of Denmark, Roskilde, Denmark, Technical Report Riso-R-1617(EN), July 2007.

30. R. Teodorescu, M. Liserre, and P. Rodriguez, *Grid Converters for Photovoltaic and Wind Power Systems*. Chichester, UK: Wiley-IEEE Press, January 2011.

31. S. Papathanassiou and M. Papadopoulos, "Mechanical stresses in fixed-speed wind turbines due to network disturbances," *IEEE Transactions on Energy Conversion*, vol. 16, no. 4, pp. 361–367, December 2001.

32. M. Hossain, H. Pota, V. Ugrinovskii, and R. Ramos, "Simultaneous STATCOM and pitch angle control for improved LVRT capability of fixed-speed wind turbines," *IEEE Transactions on Sustainable Energy*, vol. 1, no. 3, pp. 142–151, October 2010.

33. R. Pena, J. Clare, and G. Asher, "Doubly fed induction generator using back-to-back PWM converters and its application to variable-speed wind-energy generation," *IET Electric Power Applications*, vol. 143, no. 3, pp. 231–241, May 1996.

34. S. Muller, M. Deicke, and R. De Doncker, "Doubly fed induction generator systems for wind turbines," *IEEE Industry Applications Magazine*, vol. 8, no. 3, pp. 26–33, May 2002.

35. J. Ekanayake and N. Jenkins, "Comparison of the response of doubly fed and fixed-speed induction generator wind turbines to changes in network frequency," *IEEE Transactions on Energy Conversion*, vol. 19, no. 4, pp. 800–802, December 2004.

36. R. Cardenas, R. Pena, S. Alepuz, and G. Asher, "Overview of control systems for the operation of DFIGs in wind energy applications," *IEEE Transactions on Industrial Electronics*, vol. 60, no. 7, pp. 2776–2798, July 2013.

37. J. Carrasco, L. Franquelo, J. Bialasiewicz, E. Galvan, R. Guisado, M. Prats, J. Leon, and N. Moreno-Alfonso, "Power-electronic systems for the grid integration of renewable energy sources: A survey," *IEEE Transactions on Industrial Electronics*, vol. 53, no. 4, pp. 1002–1016, June 2006.

38. J. Conroy and R. Watson, "Frequency response capability of full converter wind turbine generators in comparison to conventional generation," *IEEE Transactions on Power Systems*, vol. 23, no. 2, pp. 649–656, May 2008.

39. A. S. Mikhail, K. L. Cousineau, L. H. Howes, E. William, and H. William, "Variable speed distributed drive train wind turbine system," May 2006, United States Patent, US 7,042,110 B2.

40. J. Kang, N. Takada, E. Yamamoto, and E. Watanabe, "High power matrix converter for wind power generation applications," in *International Conference on Power Electronics and Energy Conversion Congress and Exposition Asia*, Jeju, South Korea, June 2011, pp. 1331–1336.

41. S. Kouro, M. Malinowski, K. Gopakumar, J. Pou, L. Franquelo, B. Wu, J. Rodríguez, M. Perez, and J. Leon, "Recent advances and industrial applications of multilevel converters," *IEEE Transactions on Industrial Electronics*, vol. 57, no. 8, pp. 2553–2580, August 2010.

42. G. Abad, J. Lopez, M. Rodriguez, L. Marroyo, and G. Iwanski, *Doubly Fed Induction Machine: Modeling and Control for Wind Energy Generation Applications*, ser. IEEE Press Series on Power Engineering. Wiley-IEEE Press, 2011.

43. L. Y. Pao and K. Johnson, "Control of wind turbines," *IEEE Control Systems Magazine*, vol. 31, no. 2, pp. 44–62, April 2011.

44. S. Musunuri and H. Ginn, "Comprehensive review of wind energy maximum power extraction algorithms," in *IEEE Power and Energy Society (PES) General Meeting*, San Diego, CA, USA, July 2011, pp. 1–8.

45. M. Abdullah, A. Yatim, C. Tan, and R. Saidur, "A review of maximum power point tracking algorithms for wind energy systems," *Renewable and Sustainable Energy Reviews*, vol. 16, no. 5, pp. 3220–3227, 2012.

46. E. Koutroulis and K. Kalaitzakis, "Design of a maximum power tracking system for wind-energy-conversion applications," *IEEE Transactions on Industrial Electronics*, vol. 53, no. 2, pp. 486–494, April 2006.

47. K. Tan and S. Islam, "Optimum control strategies in energy conversion of PMSG wind turbine system without mechanical sensors," *IEEE Transactions on Energy Conversion*, vol. 19, no. 2, pp. 392–399, June 2004.

48. P. Cortes, M. Kazmierkowski, R. Kennel, D. Quevedo, and J. Rodríguez, "Predictive control in power electronics and drives," *IEEE Transactions on Industrial Electronics*, vol. 55, no. 12, pp. 4312–4324, December 2008.

49. A. Linder, R. Kanchan, R. Kennel, and P. Stolze, *Model-Based Predictive Control of Electric Drives*. Germany: Cuvillier Verlag Göttingen, 2010.

50. M. Kazmierkowski and L. Malesani, "Current control techniques for three-phase voltage-source PWM converters: a survey," *IEEE Transactions on Industrial Electronics*, vol. 45, no. 5, pp. 691–703, October 1998.

51. V. Yaramasu, B. Wu, S. Alepuz, and S. Kouro, "Predictive control for low-voltage ride-through enhancement of three-level-boost and NPC-converter-based PMSG wind turbine," *IEEE Transactions on Industrial Electronics*, vol. 61, no. 12, pp. 6832–6843, December 2014.

52. J. H. Lee, "Model predictive control: Review of the three decades of development," *International Journal of Control, Automation and Systems*, vol. 9, no. 3, pp. 415–424, 2011.

53. J. Rodríguez, J. Pontt, C. A. Silva, P. Correa, P. Lezana, P. Cortes, and U. Ammann, "Predictive current control of a voltage source inverter," *IEEE Transactions on Industrial Electronics*, vol. 54, no. 1, pp. 495–503, February 2007.

54. S. Kouro, P. Cortes, R. Vargas, U. Ammann, and J. Rodríguez, "Model predictive control-A simple and powerful method to control power converters," *IEEE Transactions on Industrial Electronics*, vol. 56, no. 6, pp. 1826–1838, June 2009.

55. S. Vazquez, A. Marquez, R. Aguilera, D. Quevedo, J. Leon, and L. Franquelo, "Predictive optimal switching sequence direct power control for grid-connected power converters," *IEEE Transactions on Industrial Electronics*, vol. 62, no. 4, pp. 2010–2020, April 2015.

56. L. Tarisciotti, P. Zanchetta, A. Watson, J. Clare, M. Degano, and S. Bifaretti, "Modulated model predictive control for a three-phase active rectifier," *IEEE Transactions on Industry Applications*, vol. 51, no. 2, pp. 1610–1620, March 2015.

57. M. Rivera, M. Perez, V. Yaramasu, B. Wu, L. Tarisciotti, P. Zanchetta, and P. Wheeler, "Modulated model predictive control (M^2PC) with fixed switching frequency for an NPC converter," in *International Conference on Power Engineering, Energy and Electtical Drives (POWERENG)*, Riga, Latvia, May 2015, pp. 623–628.

58. J. Rubinic, V. Yaramasu, B. Wu, and N. Zargari, "Model predictive control of neutral-point clamped inverter with harmonic spectrum shaping," in *IEEE Energy Conversion Congress and Exposition (ECCE)*, Montreal, Canada, September 2015, pp. 717–722.

59. R. Aguilera, P. Lezana, and D. Quevedo, "Switched model predictive control for improved transient and steady-state performance," *IEEE Transactions on Industrial Informatics*, vol. 11, no. 4, pp. 968–977, August 2015.

60. G. Buja and M. Kazmierkowski, "Direct torque control of PWM inverter-fed AC motors - a survey," *IEEE Transactions on Industrial Electronics*, vol. 51, no. 4, pp. 744–757, August 2004.

61. D. Casadei, F. Profumo, G. Serra, and A. Tani, "FOC and DTC: two viable schemes for induction motors torque control," *IEEE Transactions on Power Electronics*, vol. 17, no. 5, pp. 779–787, September 2002.

62. E. Fuentes, D. Kalise, J. Rodriguez, and R. Kennel, "Cascade-free predictive speed control for electrical drives," *IEEE Transactions on Industrial Electronics*, vol. 61, no. 5, pp. 2176–2184, May 2014.

63. J. Rodríguez, M. P. Kazmierkowski, J. R. Espinoza, P. Zanchetta, H. Abu-Rub, H. A. Young, and C. A. Rojas, "State of the art of finite control set model predictive control in power electronics," *IEEE Transactions on Industrial Informatics*, vol. 9, no. 2, pp. 1003–1016, May 2013.

64. V. Yaramasu, B. Wu, and J. Chen, "Model-predictive control of grid-tied four-level diode-clamped inverters for high-power wind energy conversion systems," *IEEE Transactions on Power Electronics*, vol. 29, no. 6, pp. 2861–2873, June 2014.

65. P. Cortes, S. Kouro, B. La Rocca, R. Vargas, J. Rodríguez, J. Leon, S. Vazquez, and L. Franquelo, "Guidelines for weighting factors design in model predictive control of power converters and drives," in *IEEE International Conference on Industrial Technology (ICIT)*, Gippsland, VIC, Australia, February 2009, pp. 1–7.

66. H. Miranda, P. Cortes, J. Yuz, and J. Rodríguez, "Predictive torque control of induction machines based on state-space models," *IEEE Transactions on Industrial Electronics*, vol. 56, no. 6, pp. 1916–1924, June 2009.

67. M. Chinchilla, S. Arnaltes, and J. Burgos, "Control of permanent-magnet generators applied to variable-speed wind-energy systems connected to the grid," *IEEE Transactions on Energy Conversion*, vol. 21, no. 1, pp. 130–135, March 2006.

68. J. Rodríguez, M. Rivera, J. Kolar, and P. Wheeler, "A review of control and modulation methods for matrix converters," *IEEE Transactions on Industrial Electronics*, vol. 59, no. 1, pp. 58–70, January 2012.